

# Image Cover Sheet

**CLASSIFICATION**

UNCLASSIFIED

**SYSTEM NUMBER**

515214

**TITLE**

Investigation of plastic zone development in dynamic tear test specimens -  
phase II

**System Number:****Patron Number:****Requester:****Notes:****DSIS Use only:****Deliver to:**

*This page is left blank*

*This page is left blank*

---



National Defence  
Research and  
Development Branch

Défense nationale  
Bureau de recherche  
et développement

**DREA CR 2000-115**

Sept 2000

# **INVESTIGATION OF PLASTIC ZONE DEVELOPMENT IN DYNAMIC TEAR TEST SPECIMENS – PHASE II**

T.S. Koko B.K. Gallant S.M. Tobin

MARTEC Ltd.  
400-1888 Brunswick Street  
Halifax Nova Scotia Canada  
B3J 3J8

---

## **CONTRACTOR REPORT**

---

Prepared for

Defence  
Research  
Establishment  
Atlantic



Centre de  
Recherches pour la  
Défense  
Atlantique

**Canada**

THIS IS AN UNEDITED REPORT ON SCIENTIFIC OR TECHNICAL WORK  
CONTRACTED BY THE DEFENCE RESEARCH ESTABLISHMENT ATLANTIC  
OF DEFENCE R&D CANADA.

THE CONTENTS OF THE REPORT ARE THE RESPONSIBILITY OF THE  
CONTRACTOR, AND DO NOT NECESSARILY REFLECT THE OFFICIAL  
POLICIES OF THE DEPARTMENT OF NATIONAL DEFENCE.

PLEASE DIRECT ENQUIRIES TO:

THE DIRECTOR GENERAL  
DEFENCE RESEARCH ESTABLISHMENT ATLANTIC  
P.O. BOX 1012  
DARTMOUTH, NOVA SCOTIA, CANADA  
B2Y 3Z7

## **REPRODUCTION QUALITY NOTICE**

**This document is the best quality available. The copy furnished to DRDCIM contained pages that may have the following quality problems:**

- : Pages smaller or Larger than normal**
- : Pages with background colour or light coloured printing**
- : Pages with small type or poor printing; and or**
- ✓: Pages with continuous tone material or colour photographs**

**Due to various output media available these conditions may or may not cause poor legibility in the hardcopy output you receive.**

**☒ If this block is checked, the copy furnished to DRDCIM contained pages with colour printing, that when reproduced in Black and White, may change detail of the original copy.**



National Defence  
Research and  
Development Branch

Défense nationale  
Bureau de recherche  
et développement

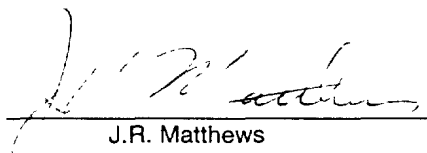
**DREA CR 2000-115**

## INVESTIGATION OF PLASTIC ZONE DEVELOPMENT IN DYNAMIC TEAR TEST SPECIMENS – PHASE II

T.S. Koko B.K. Gallant S.M. Tobin

MARTEC Ltd.  
400-1888 Brunswick Street  
Halifax Nova Scotia Canada  
B3J 3J8

Scientific Authority



J.R. Matthews

W7707-9-7208  
Contract Number

September 2000

### CONTRACTOR REPORT

Prepared for

Defence  
Research  
Establishment  
Atlantic



Centre de  
Recherches pour la  
Défense  
Atlantique

Canada

## Abstract

The development of the plastic zone in dynamic tear (DT) specimens and a non-standard three point bending fracture test specimen used to measure fracture properties was the main focus of the study. The ABAQUS finite element software was used to model the elastic-plastic behaviour of the specimens. For the DT specimen, a crack was induced by pressing the notch, followed by fatigue cracking at a limit load level of 40% of the specimen limit load, whereas, the crack shape for the non-standard specimen was a fatigue crack defined at approximately 30% of the limit load. The shapes of these cracks were adequately modelled in the finite element analysis. The specimens were made of 350WT steel and 304 stainless steel materials. The specimens were loaded until fixed amounts of permanent deformation were recorded. Results were obtained in the form of plots, showing the progression of the plastic zone around the crack tip. For each case, the results provide the following: mid point plastic deflection, stretch zone width and plastic zone radius. The finite element results obtained were compared to experimental elastic plastic testing where available, and reasonably accurate agreement was achieved.

## Executive Summary

Plastic zone size prediction is important in fracture studies because its critical value is the purest of fracture properties. All other fracture properties are related to critical plastic zone size. If you can measure and calculate the plastic zone and have determined the critical plastic zone size for the current temperature and constraint you have an accurate means of predicting failure. We are endeavouring to develop models of plastic zone in order to define the ratio of plastic zone radius to the stretch zone that develops as fracture specimens are loaded. This will aid us to define the true limits of elastic plastic testing in terms of shear lip at fracture. The models will also be used to enhance our experimental programs aimed at directly measuring plastic zone sizes by magnetic techniques.

The development of the plastic zone in dynamic tear (DT) specimens and  $B = 1/2 W$  three point bending fracture test specimens was the main focus of the study. The ABAQUS finite element software was used to model the elastic-plastic behaviour of the specimens. The specimens modelled were made of 350WT steel, the main steel on CPF ships, and 304 stainless steel, a material that lends itself to magnetic methods of viewing yielded areas. The specimens were loaded to fixed amounts of permanent deformation and plots, showing the progression of the plastic zone around the crack tip, were generated. For each case, the results provided: mid point plastic deflection, stretch zone width and plastic zone radius.

The ratios of plastic zone to stretch zone in this study did not seem particularly convincing and it is intended to expand this study to 3D and carry out a parametric study of mesh size. (original signed J.R. Matthews)

## Résumé

Le présent document porte principalement sur l'étude du développement de la zone plastique sur des éprouvettes soumises à des essais de déchirement dynamique et sur une éprouvette soumise à un essai non classique de rupture par flexion en trois points et sur son utilisation pour mesurer les propriétés de rupture. On s'est servi du logiciel d'analyse par éléments finis ABAQUS pour modéliser le comportement élastique-plastique des éprouvettes. Dans le cas du déchirement dynamique, une fissure amorcée par pression sur l'encoche s'est transformée en fissure par fatigue à 40 % de la charge limite de l'éprouvette, tandis que dans l'essai non classique, il y a eu fissuration par fatigue à environ 30 % de la charge limite. Les formes de ces fissures ont été adéquatement modélisées lors de l'analyse par éléments finis. Les éprouvettes étaient en acier 350 WT et en acier inoxydable 304. Elles ont été sollicitées jusqu'à ce qu'une quantité fixe de déformation permanente soit enregistrée. Les résultats sont présentés sous forme de graphiques montrant la progression de la zone plastique autour de la tête des fissures. Dans chaque cas, les résultats ont permis de déterminer les paramètres suivants : le fléchissement plastique au point moyen, la largeur de la zone d'allongement et le rayon de la zone plastique. Les résultats obtenus grâce à l'analyse par éléments finis ont été comparés, le cas échéant, à ceux des essais élastiques-plastiques et on a constaté une concordance assez précise.

## Sommaire

Il est important de pouvoir prédire la taille des zones élastiques quand on étudie la dynamique des ruptures, parce que la valeur critique de ce paramètre représente la forme la plus pure des propriétés de rupture. Toutes les autres propriétés de rupture sont liées à la taille des zones plastiques critiques. Si on peut mesurer et calculer la zone plastique et si on arrive à déterminer la taille de la zone plastique critique en fonction de la température et des contraintes actuelles, on dispose d'un moyen précis de prédire les défaillances. Nous avons donc cherché à développer des modèles de zone plastique afin de définir le rapport entre le rayon de la zone plastique et la zone d'allongement qui augmente à mesure que les charges sont appliquées sur les éprouvettes lors d'essais de rupture. La définition de ce paramètre nous permettra de définir les vraies limites des essais sur les propriétés élastiques et plastiques des matériaux en ce qui concerne le trait de cisaillement de la rupture. Les modèles vont aussi servir à améliorer nos programmes d'expérimentation visant à mesurer directement la taille des zones plastiques par techniques magnétiques.

L'étude a donc porté principalement sur le développement de zones plastiques sur des éprouvettes utilisées pour des essais de déchirement dynamique et sur des éprouvettes  $B = \frac{1}{2} W$  employées lors d'essais sur la rupture par flexion en trois points. Le logiciel d'analyse par éléments finis ABAQUS a été utilisé pour modéliser le comportement élastique-plastique des éprouvettes. Les éprouvettes modélisées étaient en acier 350 WT, l'acier le plus utilisé dans la construction des FCP, et en acier inoxydable 304, un matériau qui se prête bien à l'étude des zones de déformation par méthodes magnétiques. Les éprouvettes ont été soumises à des charges jusqu'à ce que des quantités fixes de déformation permanente soient enregistrées et des graphiques montrant la progression des zones plastiques autour de la tête de fissure ont été produits. Dans chaque cas, les résultats ont permis de déterminer le fléchissement plastique au point moyen, la largeur de la zone d'allongement et le rayon de la zone plastique.

Les rapports entre la zone plastique et la zone d'allongement ne sont pas convaincants et on envisage de préparer des modèles à trois dimensions pour faire une étude paramétrique de la taille du maillage.



## **ACKNOWLEDGEMENTS**

The authors would like to acknowledge the contributions of Dr. E.C. Oguejiofor of St. Francis Xavier University, Antigonish, NS and Mr. Tim Dunbar of Martec Limited, Halifax, NS.

## TABLE OF CONTENTS

<b>ABSTRACT .....</b>	<b>ii</b>
<b>ACKNOWLEDGEMENTS .....</b>	<b>iii</b>
<b>TABLE OF CONTENTS .....</b>	<b>iv</b>
<b>LIST OF FIGURES .....</b>	<b>v</b>
1. INTRODUCTION .....	1.1
1.1 Background .....	1.1
1.2 Objectives and Scope .....	1.2
2. PROBLEM DESCRIPTION.....	2.1
2.1 Specimen Configurations .....	2.1
2.2 Crack Tip Shape .....	2.1
2.3 Requirements.....	2.2
3. FINITE ELEMENT MODEL .....	3.1
3.1 Finite Element Approach .....	3.1
3.2 Finite Element Meshes .....	3.1
3.3 Material Models .....	3.1
3.3.1 350WT Steel .....	3.2
3.3.2 304 Stainless Steel .....	3.2
3.4 Boundary Conditions and Loading.....	3.3
4. RESULTS AND DISCUSSIONS.....	4.1
4.1 DT Specimen with 350 WT Steel Material.....	4.1
4.2 DT Specimen with 304 Stainless Steel Materials .....	4.2
4.3 NS Specimen with 304 Stainless Steel Material .....	4.4
5. SUMMARY, CONCLUSIONS AND RECOMMENDATIONS.....	5.1
5.1 Summary and Conclusions.....	5.1
5.2 Recommendations .....	5.2
6. REFERENCES .....	6.1

## LIST OF FIGURES-

Figure 3.1: Shape of Fatigue Crack in DT Specimens .....	3.4
Figure 3.2: FE Mesh of 8.0 mm Thick DT Specimen (a) Full Mesh (b) Close-up Mesh.....	3.5
Figure 3.3: Full FE Mesh of 12.5 mm Thick Standard Specimen .....	3.6
Figure 3.4: Full FE Mesh of 25.0 mm Thick DT Specimen.....	3.6
Figure 3.5: Stress–Strain Curve of 350WT Steel .....	3.7
Figure 3.6: Stress–Strain Curve of 304SS Steel .....	3.7
Figure 4.1: Final Displacements of DT-350WT-08 Specimen: (a) Displacement Contours; (b) Undeformed Shape Near Crack Tip; (c) Deformed Shape Near Crack Tip.....	4.7
Figure 4.2: Plastic Strain Contours in DT-350WT-08 Specimen (a) $D_L/B = 0.00340$ (b) $D_L/B = 0.00544$ .....	4.8
Figure 4.3: Plastic Strain Contours in DT-304SS-08 Specimen (a) $D_L/B = 0.00340$ (b) $D_L/B = 0.00544$ .....	4.11
Figure 4.4: von Mises Stress Contours in DT-350WT-08 Specimen (a) $D_L/B = 0.00544$ (b) $D_L/B = 0.02724$ .....	4.14
Figure 4.5: von Mises Stress Contours in DT-304SS-08 Specimen (a) $D_L/B = 0.00544$ (b) $D_L/B = 0.02724$ .....	4.16
Figure 4.6: Plastic Strain Contours in NS-350WT-12 Specimen (a) $D_L/B = 0.00250$ (b) $D_L/B = 0.00401$ .....	4.18
Figure 4.7: Plastic Strain Contours in NS-304SS-12 Specimen (a) $D_L/B = 0.00250$ (b) $D_L/B = 0.00421$ .....	4.21
Figure 4.8: von Mises Stress Contours in NS-350WT-12 Specimen (a) $D_L/B = 0.00401$ (b) $D_L/B = 0.02505$ .....	4.24
Figure 4.9: von Mises Stress Contours in NS-304SS-12 Specimen (a) $D_L/B = 0.00421$ (b) $D_L/B = 0.02532$ .....	4.26
Figure 4.10: Plastic Strain Contours in DT-350WT-25 Specimen (a) $D_L/B = 0.00111$ (b) $D_L/B = 0.00178$ .....	4.28
Figure 4.11: Plastic Strain Contours in DT-304SS-25 Specimen (a) $D_L/B = 0.00111$ (b) $D_L/B = 0.00178$ .....	4.31
Figure 4.12: von Mises Stress Contours in DT-350WT-25 Specimen (a) $D_L/B = 0.00178$ (b) $D_L/B = 0.01113$ .....	4.34
Figure 4.13: von Mises Stress Contours in DT-304SS-25 Specimen (a) $D_L/B = 0.00178$ (b) $D_L/B = 0.01113$ .....	4.36
Figure 4.14: Variation of Maximum Plastic Strain with Non-Dimensionalized Displacement for all Specimens.....	4.38
Figure 4.15: Schematic Illustration of Plastic Radius ( $r_p$ ) and Stretch Zone Width (SZW) ...	4.38
Figure 4.16: Variation of Plastic Radius with Non-Dimensionalized Displacement for all Specimens .....	4.39
Figure 4.17: Variation of SZW with Non-Dimensionalized Displacement for all Specimens .....	4.39
Figure 4.18: Variation of $r_p$ /SZW with Non-Dimensionalized Displacement for all Specimens (a) Actual Data (b) Data Trend .....	4.40

## **1. INTRODUCTION**

### **1.1 Background**

This study is a continuation of an effort to provide an understanding of the ratio of crack tip blunting (stretch zone) to the plastic zone size (radius) in order to determine the upper limit of temperature relative to full size transition curves where elastic plastic fracture becomes invalid. The finite element (FE) technique is used to provide this ratio and the results of interest in the proposed work is the investigation of the development of the plastic zone in dynamic tear (DT) test specimens and a non-standard specimen. The dynamic tear test involves a single-edge notched beam that is impact loaded in three-point bending, and the DT energy, which is a measure of resistance to rapid progressive fracturing, is recorded. The specimens are fractured with drop-weight machines. The size and shape of the plastic zone, the stretch zone and the shear lips that form are important parameters that can be used to develop analytical models for describing the material behaviour.

In the Phase I study [1], the finite element methodology was utilized to provide an understanding of the plastic zone size (radius) to crack tip blunting (stretch zone width). Finite element analyses of three test specimen configurations were performed. The test specimens were (i) a standard dynamic tear (DT) test specimen with 350WT steel; (ii) another standard DT specimen with 304 stainless steel; and (iii) a non-standard three point bend specimen with 304 stainless steel. The ABAQUS finite element code was used to perform incremental elastic-plastic analysis of the specimens. Intuition and experimental observation were used to develop approximate stress-strain curves for the materials beyond the points where uniaxial stress-strain data were available for the 350WT steel and 304 stainless steel materials. Results computed included the midpoint displacement; development of the plastic zone around the crack tip with progression of load; the plastic zone radius  $r_p$ ; stretch zone width (SZW); and the ratio of plastic zone radius to SZW. The results were presented in the form of contour plots and charts. The goal of the present study is to continue the Phase I work in order to provide better accuracy and to apply the methodology to other DT specimen configurations. The methodology is applied to two DT and one non-standard test specimens made of 350WT and 304SS materials.

## 1.2 Objectives and Scope

Comparison of the finite element results with experimental results could not be made in the Phase I study as these were being performed concurrently. Consequently, the full stress-strain relations used in the Phase I study were based on intuition and limited experimental observations. The full stress-strain relations for the 350WT and 304SS materials are now available from the experimental investigations and would be used for the finite element models, in order to facilitate suitable comparisons of the finite element results to experimental observations. Using these material relations, the finite element methodology is applied to three specimen configurations, including (i) the standard DT specimen with a width of 41mm and 8mm thickness, (ii) the non-standard (NS) specimen, and (iii) another DT specimen with a width of 50 mm and thickness of 25 mm.

Chapter 2 provides detailed descriptions of the specimen configurations considered in the study, and a description of the crack tip shape. The finite element methodology utilized in the investigation is presented in Chapter 3, which provides details of the finite element meshes, materials constitutive models, boundary and loading conditions, and the solution methodology. The finite element results are presented in Chapter 4, with discussions of the results. Finally, Chapter 5 provides a summary of the study and the conclusions reached.

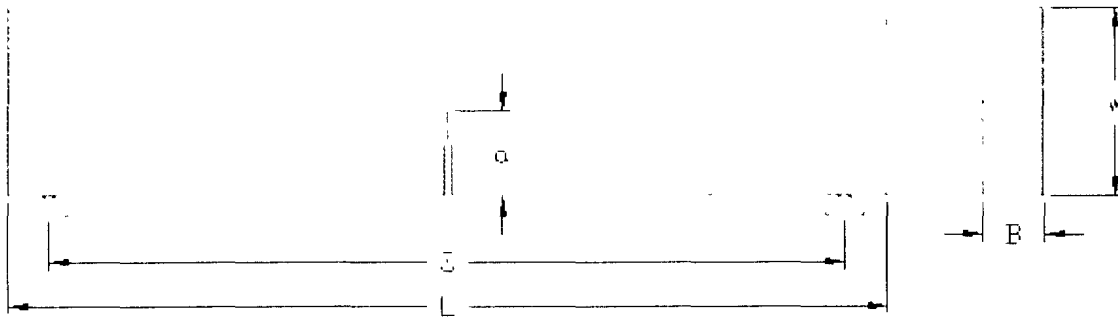


Figure 2.1: Configuration of DT Specimen

## **2. PROBLEM DESCRIPTION**

### **2.1 Specimen Configurations**

A schematic representation of the test specimen is presented in Figure 2.1. In the present study, six test configurations are analyzed. These include the following:

- (i) DT specimen, 350WT material, 8 mm thickness (designated as DT-350WT-08);
- (ii) DT specimen, 304SS material, 8 mm thickness (designated as DT-304SS-08);
- (iii) NS specimen, 350WT material, 12.5 mm thickness (designated as NS-350WT-12);
- (iv) NS specimen, 304SS material, 12.5 mm thickness (designated as NS-304SS-12);
- (v) DT specimen, 350WT material, 25 mm thickness, 50 mm width (designated as DT-350WT-25); and
- (vi) DT specimen, 304SS material, 25 mm thickness, 50 mm width (designated as DT-304SS-25).

The dimensions of the specimens are shown in Table 2.1.

### **2.2 Crack Tip Shape**

The crack tip shape is that of a fatigue crack initially and a blunted fatigue crack thereafter. For the DT specimen the notch is first machined with an included angle of  $60^\circ$  followed by a pressing process that extends the notch 0.254 mm (0.010) with an included angle of  $40^\circ$  and a resulting crack tip radius of 0.254 mm (0.001). This is followed by fatigue cracking at a load level of no more than 40% of the current specimen limit load. This produces a sharp fatigue crack of definable dimensions, which we would like to use in the FE simulation. This pre-cracking extends the pressed notch by at least 1 mm.

The crack tip shape for the non-standard specimen is that of a well established fatigue crack whose maximum loading has been defined by careful laboratory fatiguing (maximum load approximately 30% of the limit load). The shape of the resulting crack tip and the configuration of the crack along its entire length were acquired by sectioning. Changes in shape of the crack tip as the FE model is run from one plastic boundary condition to another are compared to detailed laboratory metallographic measurements. Detailed descriptions of the precracking process is available in Reference [2].

### 2.3 Requirements

It was required to compute the progression of the plastic zone around the crack tip under quasi-static loading conditions, for the three specimens. For each case, the following response parameters were required:

- (i) Progression of plastic zone around the crack tip, including contour plots of plastic strain;
- (ii) Midpoint plastic deflections;
- (iii) Stretch zone width (i.e. distance from crack tip to interface of yield zone with side of crack);
- (iv) Plastic zone radius (i.e. locus and maximum extent of plastic zone); and
- (v) Charts of SZW, plastic zone radius  $r_y$  and ratio of SZW/ $r_y$  for various plastic loading conditions.

Table 2.1: Dimensions of Specimens

Dimensions	Specimen		
	Standard DT	Non-Standard	DT with 1" x 2" Bar
Beam Length, L (mm)	181.00	125.00	225.00
Beam Span, S (mm)	164.00	100.00	200.00
Crack Length, a (mm)	14.00*	12.50**	14.00*
Beam Width, W (mm)	41.00	25.00	50.00
Beam Thickness, B (mm)	8.00	12.50	25.00

\*a = 12 mm plus 0.254 mm pressing followed by fatigue extension to 14 mm

\*\*a = 12.5 mm fatigue crack produced by rigorous process



### **3. FINITE ELEMENT MODEL**

#### **3.1 Finite Element Approach**

The ABAQUS finite element software [3] was used to model the elastic-plastic behaviour of the DT specimen. The software has a wide range of non-linear materials models and can account for large strains and displacements. However, the HyperMesh [9] general-purpose pre- and post-processing program was used for model generation and results processing. Details of the finite element model are provided below.

#### **3.2 Finite Element Meshes**

The HyperMesh code was used to generate the finite element models of the DT and non-standard specimens, which were then translated to ABAQUS input files. The exact shapes of the crack were obtained from DREA to enable accurate modelling of the structural configuration. Figure 3.1 shows the shape of the fatigue crack in the DT specimen. This shape had to be modelled accurately to provide meaningful results. Detailed 2-D finite element models of the specimen were developed. In order to reduce the problem size only one-half of the structure was modelled using symmetry conditions. The finite element models of the DT and non-standard (NS) specimens are as shown in Figures 3.2-3.4, respectively. Four-noded plane strain elements were used to model the structure. These elements allow for the treatment of large displacements, finite strains and plasticity, which are expected to occur in the specimen. The close-up view shown in Figure 3.2 is applicable to all the specimens.

#### **3.3 Material Models**

An incremental rate independent plasticity theory available in the ABAQUS finite element program [3] was used for the material constitutive model. This standard model for plasticity is summarized in the Phase I report [1].

The Kirchhoff stress and logarithmic strain measures are employed because of advantages gained in computational implementation. The assumption is made that the structure undergoes only small changes in volume and, hence, the Kirchhoff stresses are approximately equal to the physically motivated Cauchy stresses. The uniaxial Cauchy stress-logarithmic strain constitutive response of the material are formally input, in multilinear form, as Cauchy stress and logarithmic plastic strain pairs for the ABAQUS program. The constitutive parameters for the 350WT and 304SS materials are described below.

### **3.3.1 350WT Steel**

Figure 3.5 shows the stress-strain behaviour of 350 WT steel material. As shown in the figure, data points are available up to 200% plastic strain. Recall that in the Phase I study the measured stress-strain curve terminated at 25% strain, and an approximate curve was used in the range from 25% to 250% plastic strain based on intuition and observation. It turns out that the “rising curve” model used in Phase I is actually close to the current curve. The actual stress-strain data points used for the finite element analysis are also shown in the figure. The yield stress was taken as 465 MPa. Note that beyond 200% plastic strain, the curve was assumed to be flat with the plastic strain increasing at constant plastic stress.

### **3.3.2 304 Stainless Steel**

Figure 3.6 shows the stress-strain behaviour of the 304 stainless steel material. Data points are available up to 300% plastic strain. In the Phase I study, the stress-strain behaviour was taken from the literature and it varied significantly from the current stress-strain current (with regards to the yield stress and plastic modulus). The actual stress-strain data points used for the finite element analysis are also shown in the figure. The yield stress was taken as 498 MPa. Note also that beyond 300% plastic strain, the curve was assumed to be flat with the plastic strain increasing at constant plastic stress.

### 3.4 Boundary Conditions and Loading

The following boundary conditions were applied:

At the support:  $v = 0$

Along the center line:  $u = 0$ ;

where,  $u, v$  are the displacements components in the longitudinal and transverse directions.

### 3.5 Loading

The load was applied in the form of a displacement of the top midpoint of the beam specimen. The displacement was applied incrementally in steps of about 0.0001 mm. This is different from the Phase I work in which the load was applied as a concentrated incremental load at the top middle point of the beam.

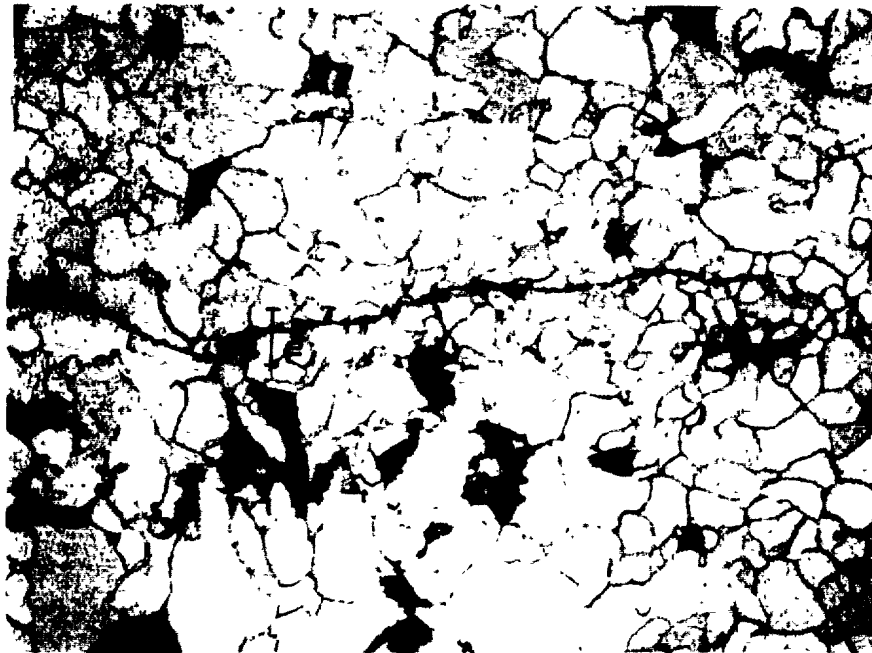
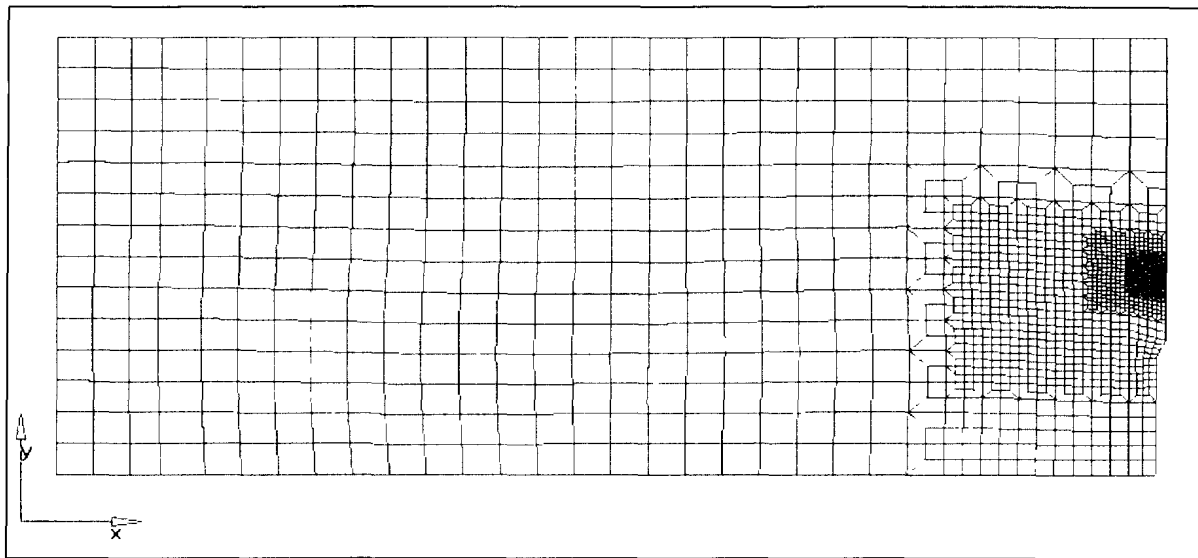
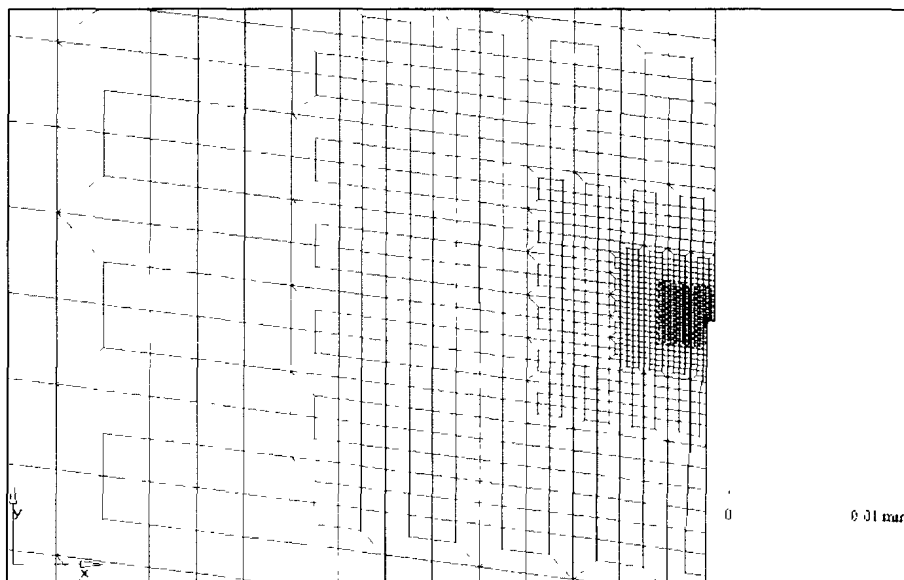


Figure 3.1: Shape of Fatigue Crack in DT Specimens



(a)



(b)

Figure 3.2: FE Mesh of 8.0 mm Thick DT Specimen (a) Full Mesh (b) Close-up Mesh

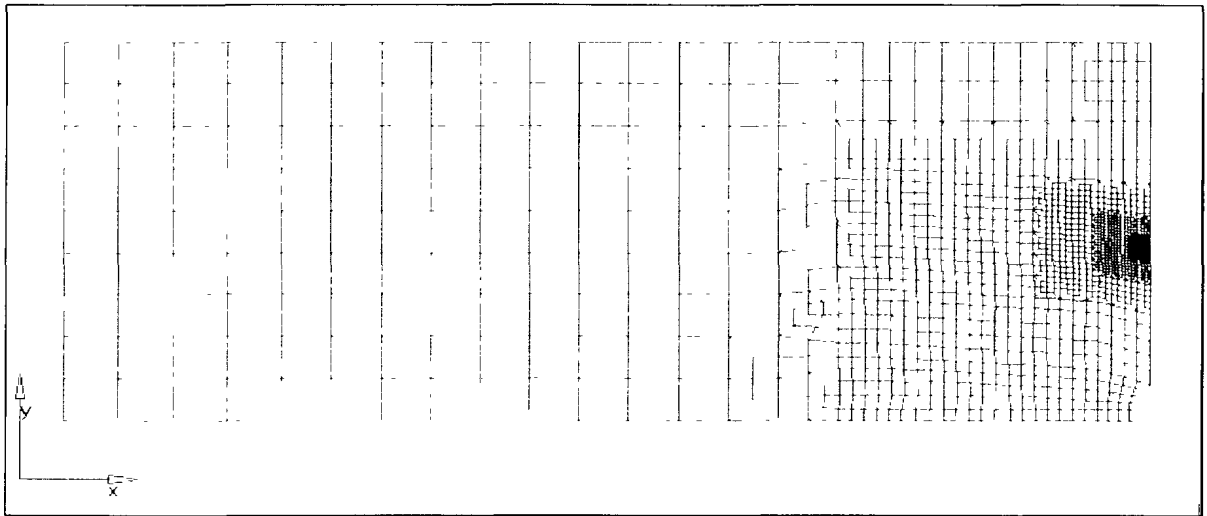


Figure 3.3: Full FE Mesh of 12.5 mm Thick Standard Specimen

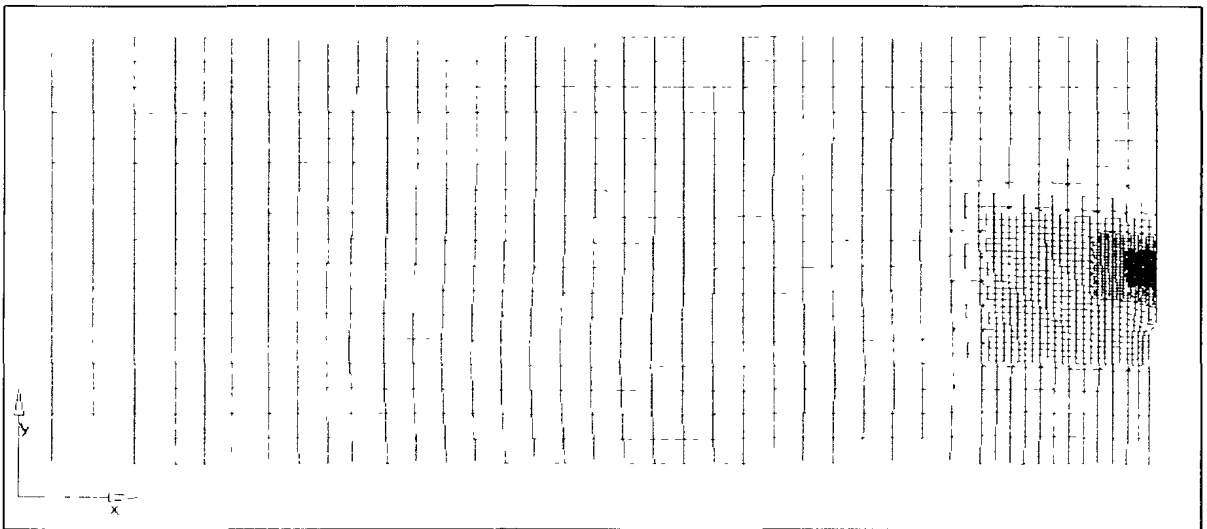


Figure 3.4: Full FE Mesh of 25.0 mm Thick DT Specimen

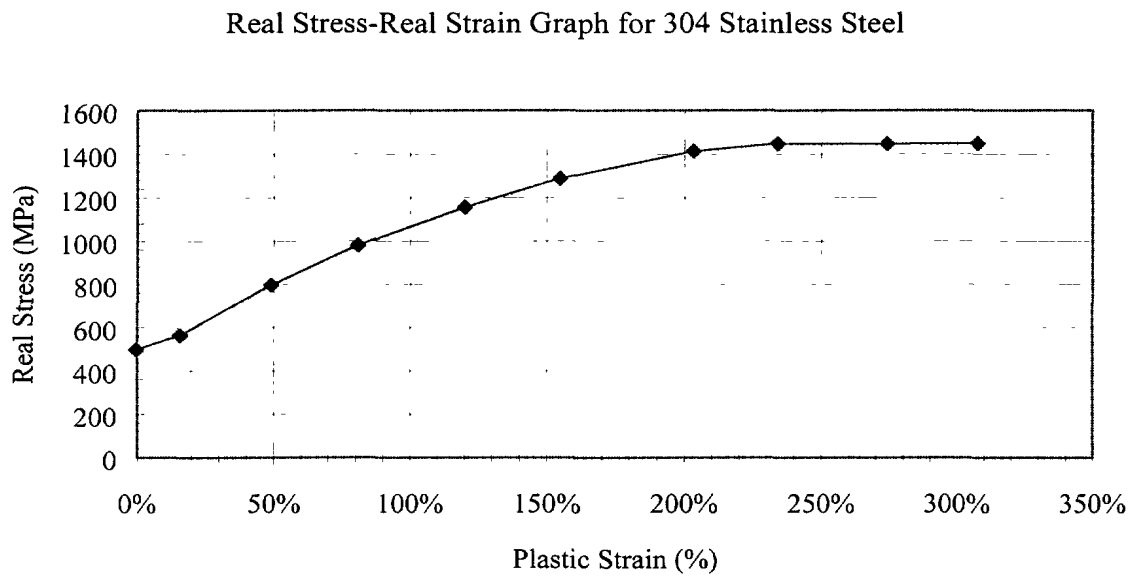


Figure 3.5: Stress–Strain Curve of 350WT Steel

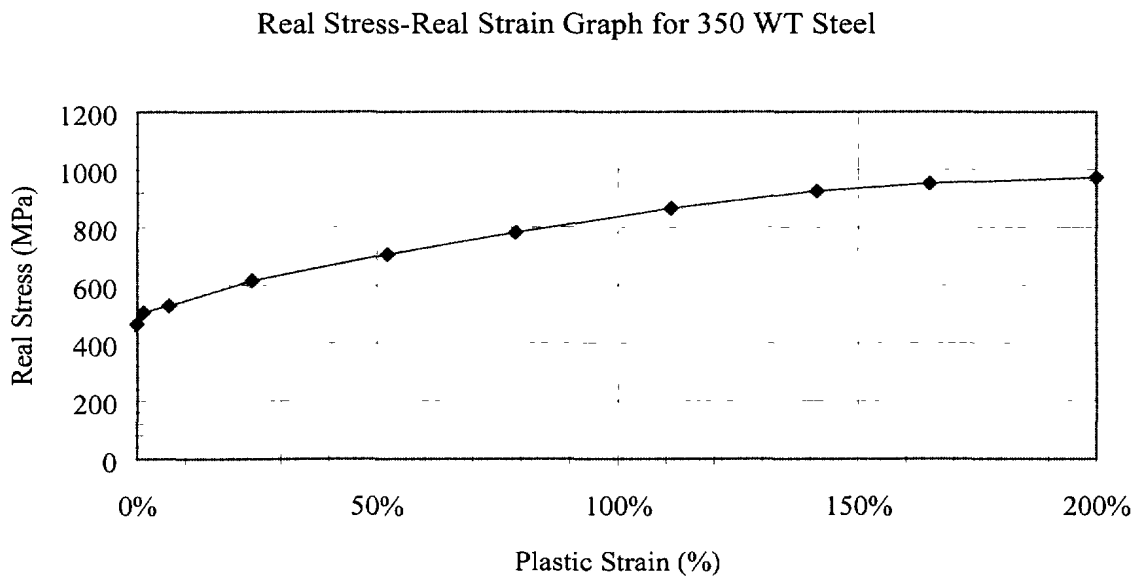


Figure 3.6: Stress–Strain Curve of 304SS Steel

## 4. RESULTS AND DISCUSSIONS

This chapter discusses the results of the study. For each specimen, results of the midpoint displacement, plastic zone development, plastic strain, plastic radius, and stretch zone width are provided in the following section.

### 4.1 Midpoint Displacements

In the Phase I study, the loading was applied in the form of an incremental concentrated load at the top midpoint of the beam, and load displacement responses of the specimens were provided [1]. In this study, the loading was applied in the form of incremental displacement at the top midpoint of the beam. Preliminary analyses were performed to ensure that the two methods provided the same results. This was accomplished by performing two analyses. In the first analysis, a predetermined load was applied incrementally and the resulting midpoint displacement, stresses and strains were noted. In the second analysis, the midpoint displacement obtained from the first analysis was applied incrementally at the top midpoint of the beam. The resulting stresses and strains were again noted and compared with those obtained from the first analysis. These appeared to be identical confirming that the two approaches provided similar results.

Figure 4.1 shows the displacement contours of the DT-350WT-08 specimen at the last displacement increment. This displacement contour pattern was observed at all displacement increments for all the specimens. Detailed deformed and undeformed plots near the crack tip of the DT-350WT-08 specimen are also shown in the Figure 4.1 illustrating the very large stretching (strain) of the elements near the crack tip. Again, this behaviour was observed for all specimens.

Table 4.1 shows the maximum midpoint displacements attained for the six specimens. These displacements are also shown in non-dimensional form with respect to the thicknesses. It is seen that although the maximum midpoint displacements applied to all the specimens are close, there is a wide variation in the values of the non-dimensional displacements due to the differences in the specimen thickness.



## 4.2 Plastic Zone Development

The development of the plastic zone around the crack tip was determined using contour plots of the equivalent plastic strain or von Mises stress at various steps of the loaded. As was noted in the Phase I study, the shapes and sizes of the plastic zones using the von Mises stress or equivalent stress are very similar.

### *DT Specimens with 8mm Thickness*

Figures 4.2 and 4.3 show the plastic strain contours at various displacement levels in the DT-350WT-08 and DT-304SS-08 specimens, respectively. Note that different scales are used to plot the contours at different load levels due to the differences in the magnitudes of the strains at the various levels. However, it is seen that for a given specimen the size of the plastic zone as well as the magnitude of the maximum plastic strains increase with the applied displacement. It is also seen that the shape of the plastic strain contours for the DT-350WT-08 and DT-304SS-08 specimens are similar, as expected, since they both have the same dimensions, but differ only in the material (350WT steel or 304 Stainless Steel). The 304SS material has a slightly higher yield stress (498 MPa compared to 465 MPa for 350WT), as well as a slightly high plastic modulus (see Figures 3.5 and 3.6). Therefore, at similar plastic displacement-to-thickness ( $d/B$ ) ratios, during the early stages of the loading, the magnitudes of the plastic strain in the two specimens were very close, with those of the 304SS material being slightly smaller. However, at the later stages of the loading, differences in the magnitudes of the maximum plastic strain become more significant. Thus, the 304SS specimen can sustain significantly higher strains should more load be applied to the structures.

### *NS Specimens*

Figures 4.4 and 4.5 show contours of the von Mises stresses in the DT-350WT-08 and DT-304SS-08 specimens and various displacement levels. These show more clearly the plastic zones (that is areas with stress levels greater than the yield stresses). Again, the shapes of the stress contours for the 350WT and 304SS materials are very similar. Differences occur only in the magnitudes of the maximum stresses at the various displacement levels.

Figures 4.6 and 4.7 show the plastic strain contours at various displacement levels in the NS-350WT-12 and NS-304SS-12 specimens, respectively. Again, the plastic zone size increases with the applied load increment and the shape of the plastic strain contours for both specimens are very similar since they have the geometric configuration. However, the magnitudes of the maximum plastic strains in the NS-304SS-12 specimen are generally smaller than those of the NS-304SS-12 specimens at the various plastic displacement levels. As discussed earlier (for the 8mm thick DT specimens), this is due to the fact that the 304SS material had a higher yield stress than the 350WT material (498 MPa for 304SS compared to 465 MPa for 350WT), as well as higher plastic modulus. The differences in the magnitudes of the maximum plastic strain is more significant in the later stages of loading. Hence the 304SS specimen is expected to sustain significantly higher strains than the 350WT specimen, if more load is applied to the structure. At plastic displacement to thickness ( $d/B$ ) ratios of up to 0.03, the shapes of plastic strain contours for the 12.5mm thick non-standard and 8mm thick standard DT specimens are very similar. Beyond this displacement level, the plastic strain contours of the 12.5mm non-standard specimens tend to be narrower while also pointing upwards. However, the level of plastic strain reached at this point is beyond the range (200% plastic strain for 350WT and 300% plastic strain for 304SS), covered by the experimental real stress-real strain curve, the finite element model assumes that real stress-real strain behaviours of the materials undergo plastic strain at constant stress (960 MPa for 350WT and 1450 MPa for 304SS).

Figures 4.8 and 4.9 show the contours of von Mises stresses in the NS-350WT-12 and NS-304SS-12 specimens at various displacement levels. The shapes of the contours are similar for the 350WT and 304SS materials; differences occur only in the magnitudes of the stresses. As with the plastic strain contours, the plastic stress contours tend to get narrower, while also pointing more towards the beam top, at higher displacement levels.

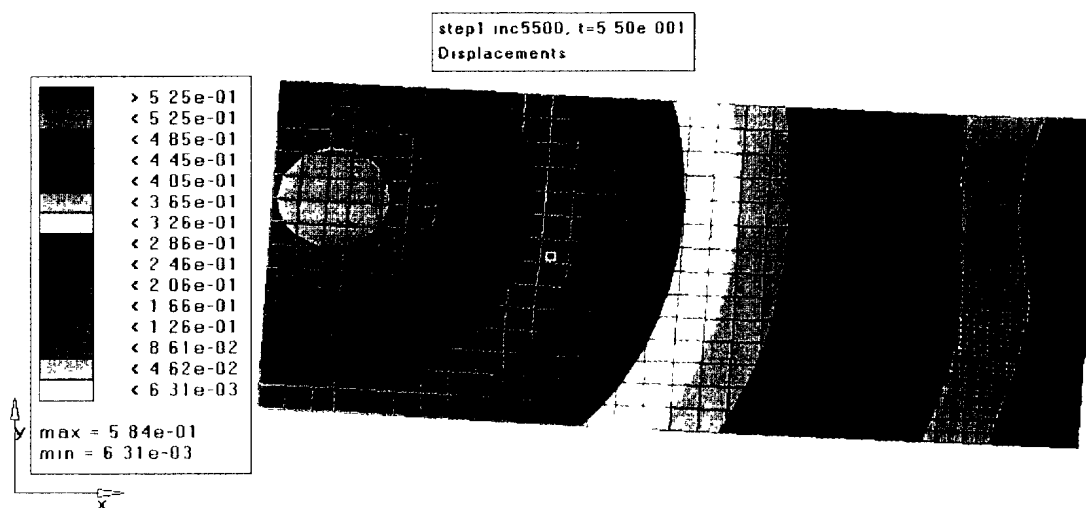
#### *DT Specimens with 25mm Thickness*

Figures 4.10 and 4.11 show the plastic strain contours at various displacement levels in the DT-350WT-25 and DT-304SS-08 specimens, respectively. As observed in the other specimens, the plastic zone size as well as the maximum plastic strains increase with the applied

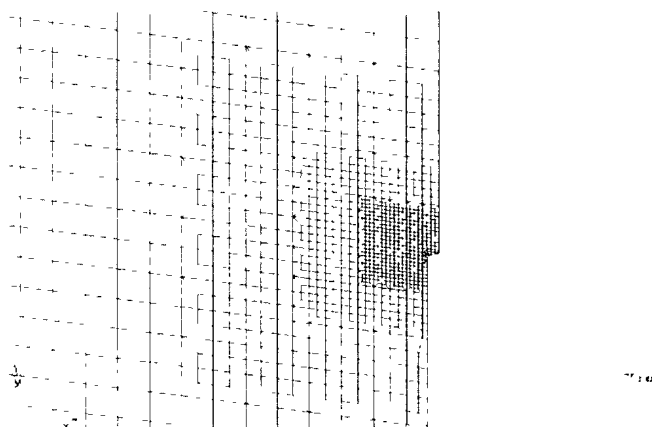
Uncertainties in the  $r_y$ /SZW ratio are invariably introduced into the solution because of uncertainties in measuring  $r_y$  and SZW. It is expected that the values of  $r_y$  and SZW are influenced by the sizes of the element around the crack tip, but this was not investigated in the study. An investigation of this is required to provide better accuracy.

Table 4.1: Maximum Midpoint Displacements Attained for Various Specimens

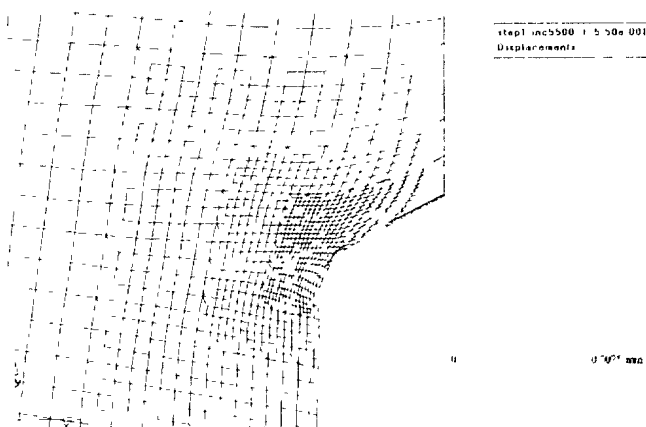
No.	Specimen	Maximum Midpoint Displacement	$D_t/B$
1	DT-350WT-08	0.616	0.0770
2	DT-304SS-08	0.557	0.0696
3	NS-350WT-12	0.685	0.0548
4	NS-304SS-12	0.616	0.0493
5	DT-350WT-25	0.689	0.0275
6	DT-304SS-25	0.665	0.0266



(a)

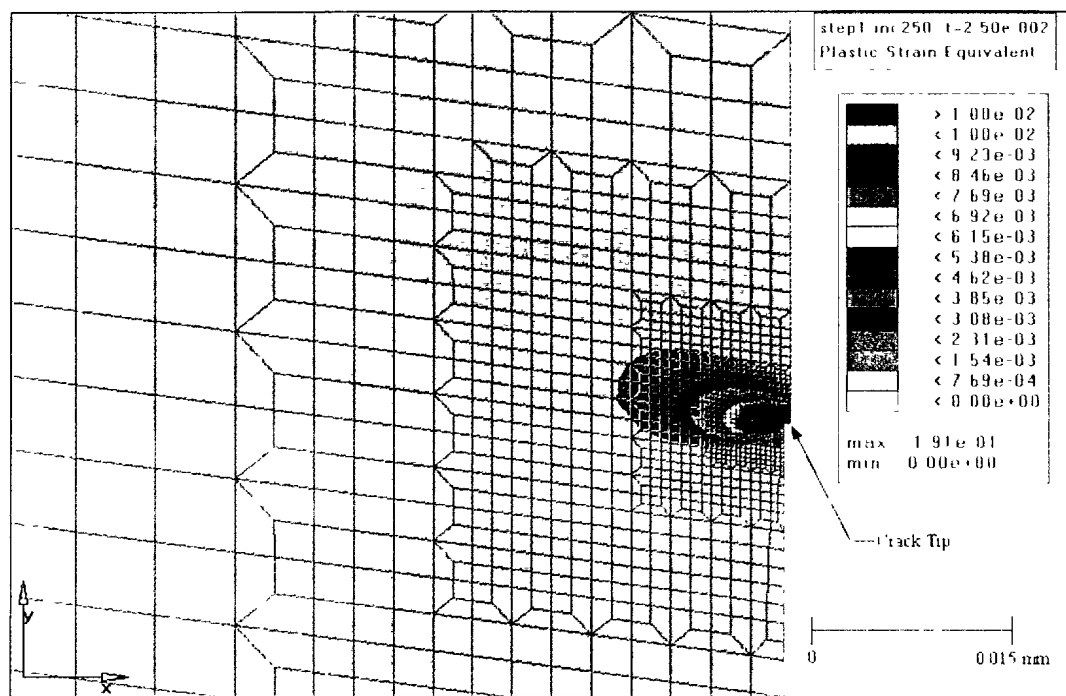


(b)

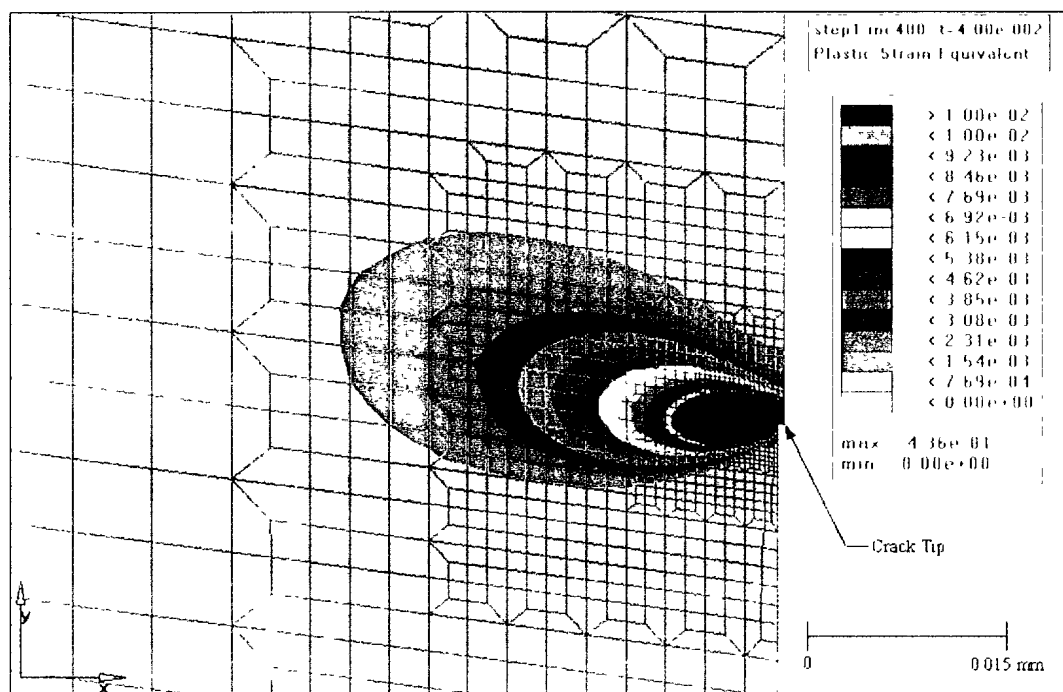


(c)

Figure 4.1: Final Displacements of DT-350WT-08 Specimen: (a) Displacement Contours; (b) Undeformed Shape Near Crack Tip; (c) Deformed Shape Near Crack Tip

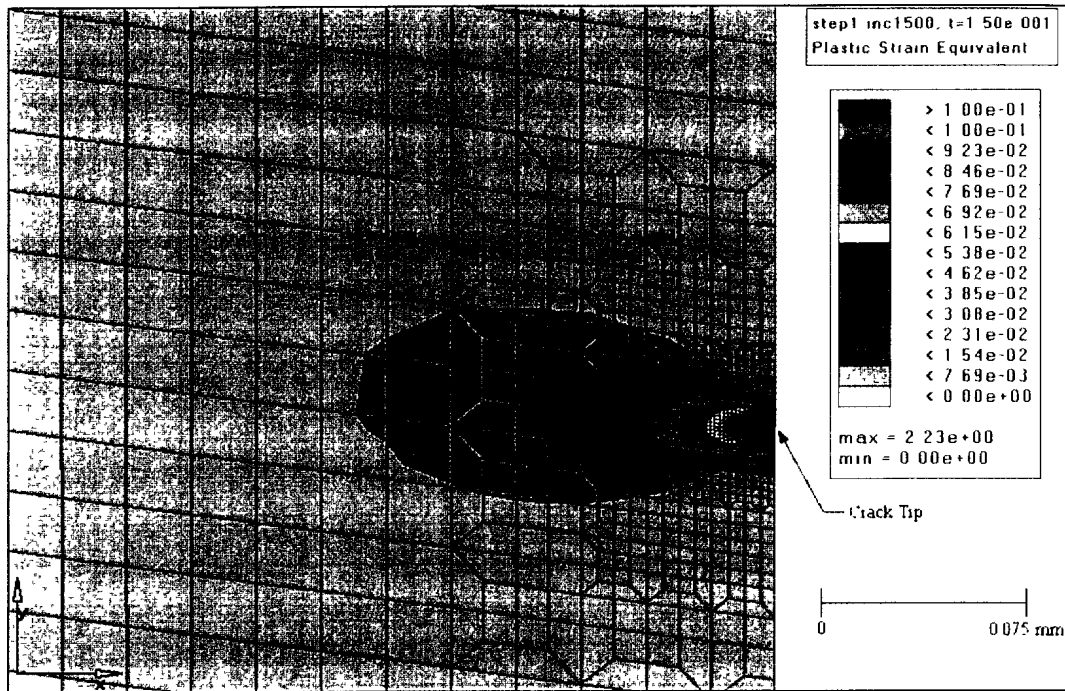


(a)

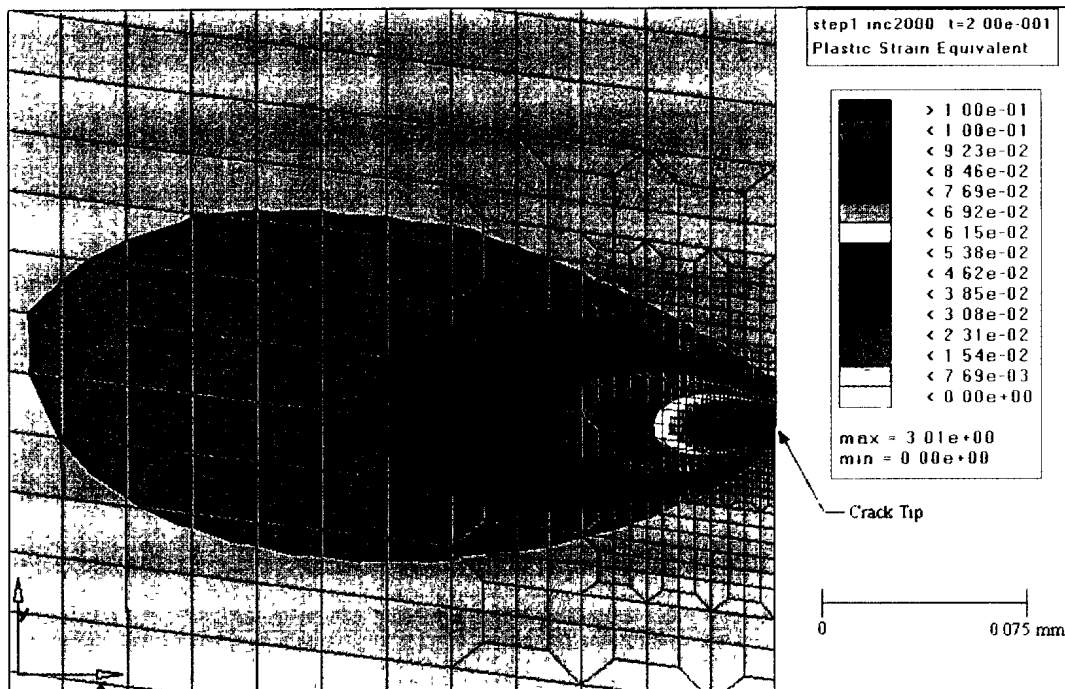


(b)

Figure 4.2: Plastic Strain Contours in DT-350WT-08 Specimen (a)  $D_L/B = 0.00340$  (b)  $D_L/B = 0.00544$

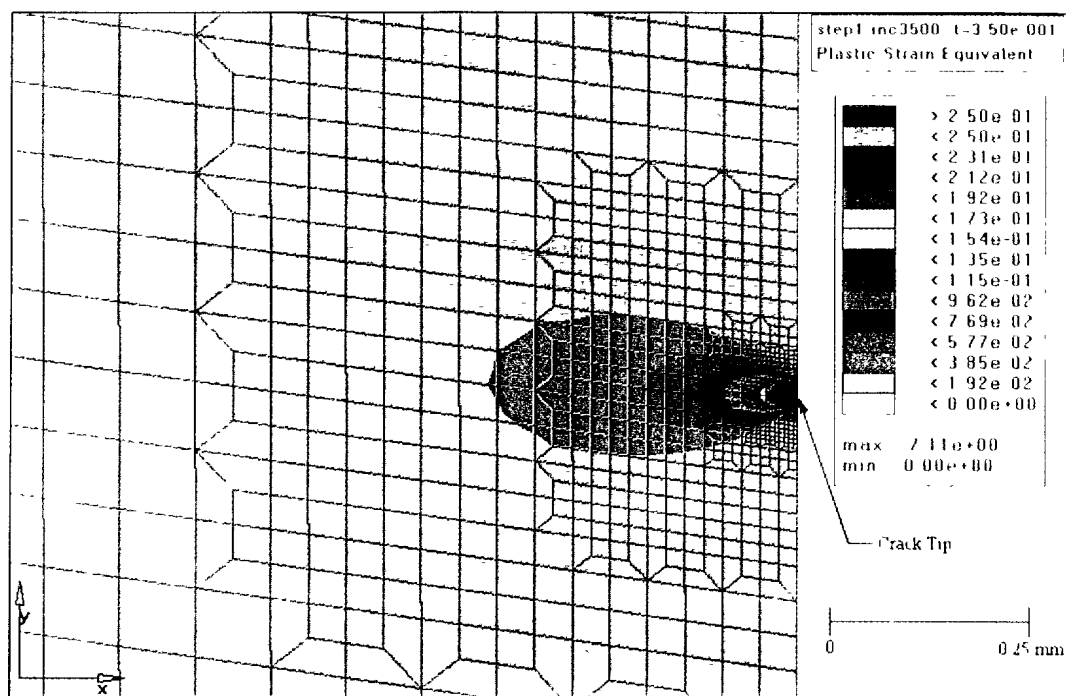


(c)

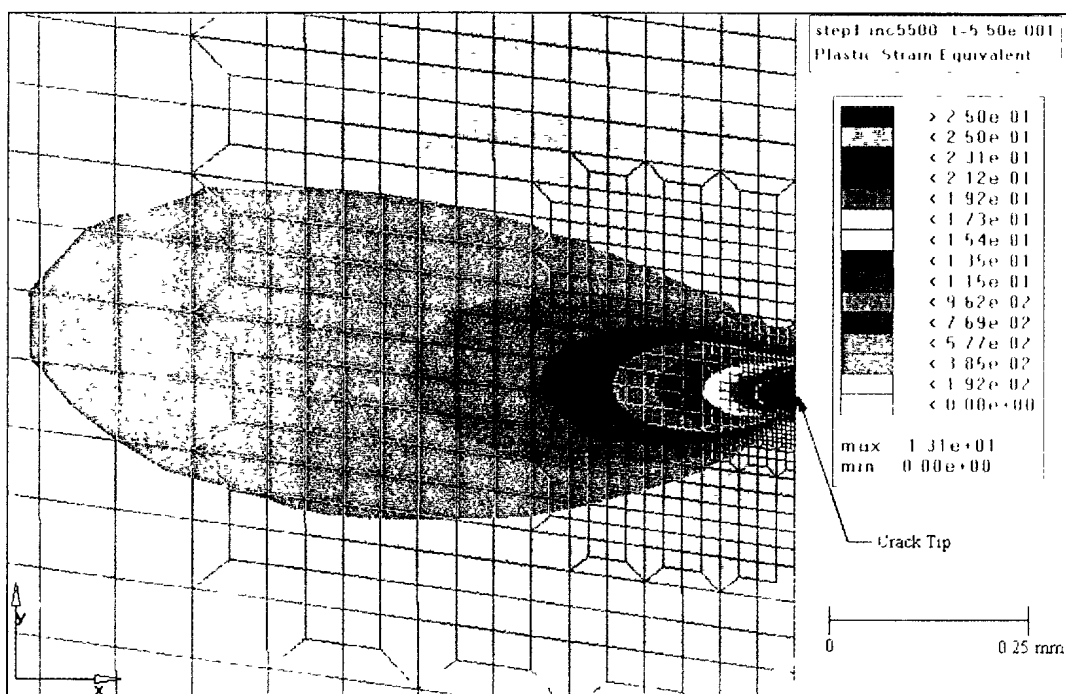


(d)

Figure 4.2 - Plastic Strain Contours in DT-350WT-08 Specimen, (c)  $D_L/B = 0.02041$  (d)  $D_L/B = 0.02724$

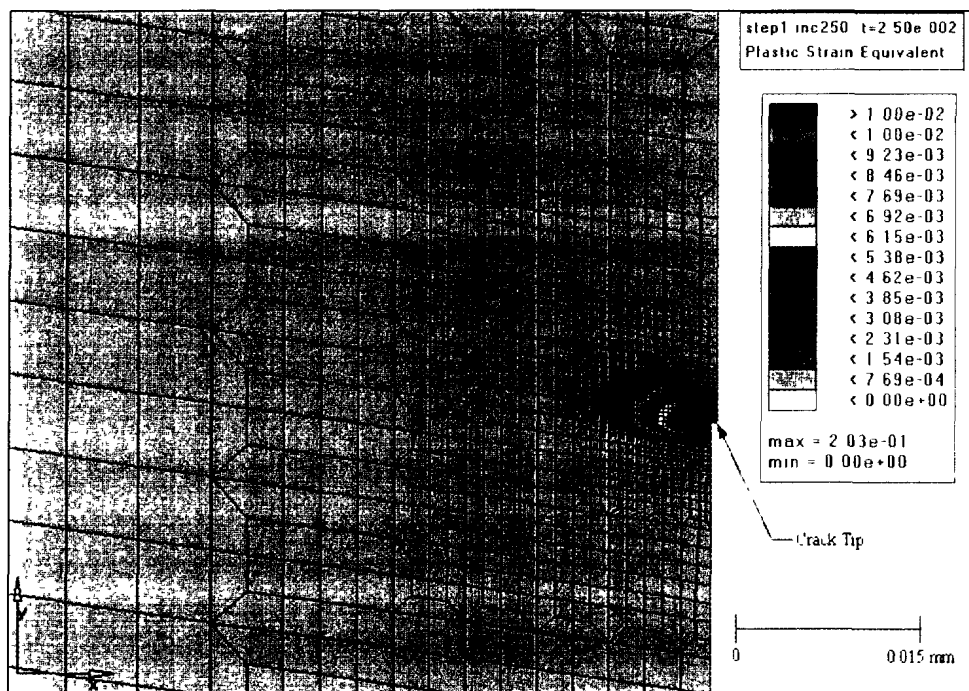


(e)

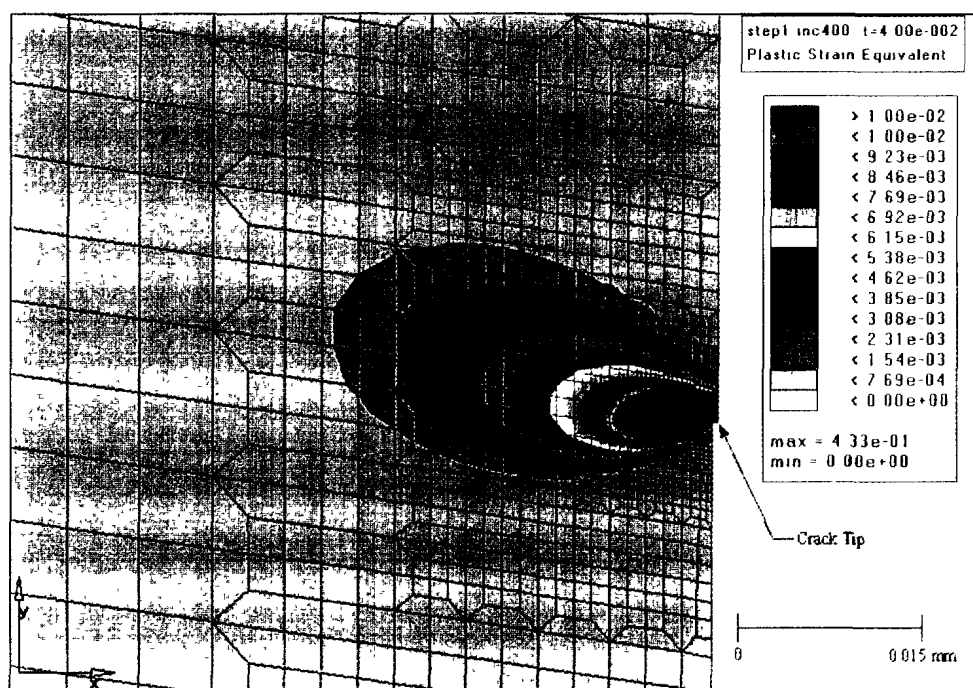


(f)

Figure 4.2 - Plastic Strain Contours in DT-350WT-08 Specimen (e)  $D_L / B = 0.04799$  (f)  $D_L / B = 0.07700$



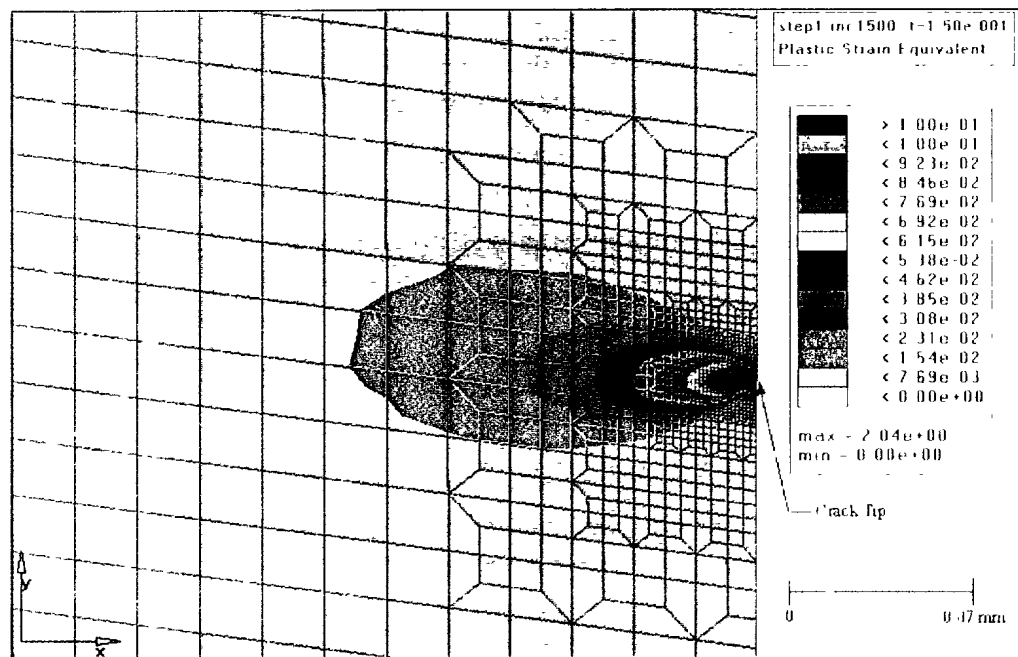
(a)



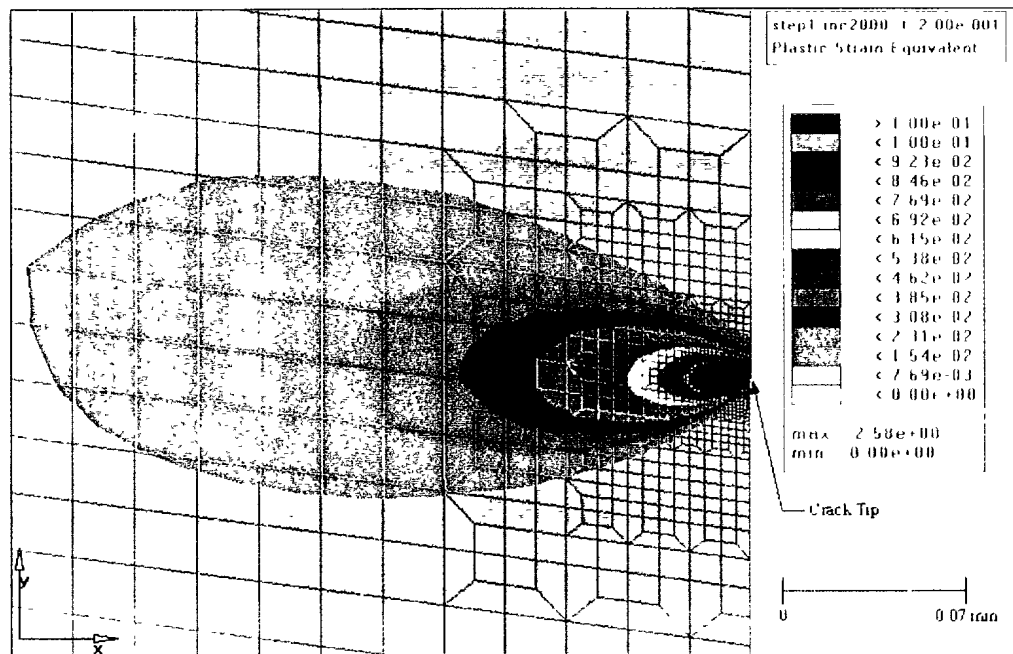
(b)

Figure 4.3: Plastic Strain Contours in DT-304SS-08 Specimen (a)  $D_L/B = 0.00340$  (b)  $D_L/B = 0.00544$



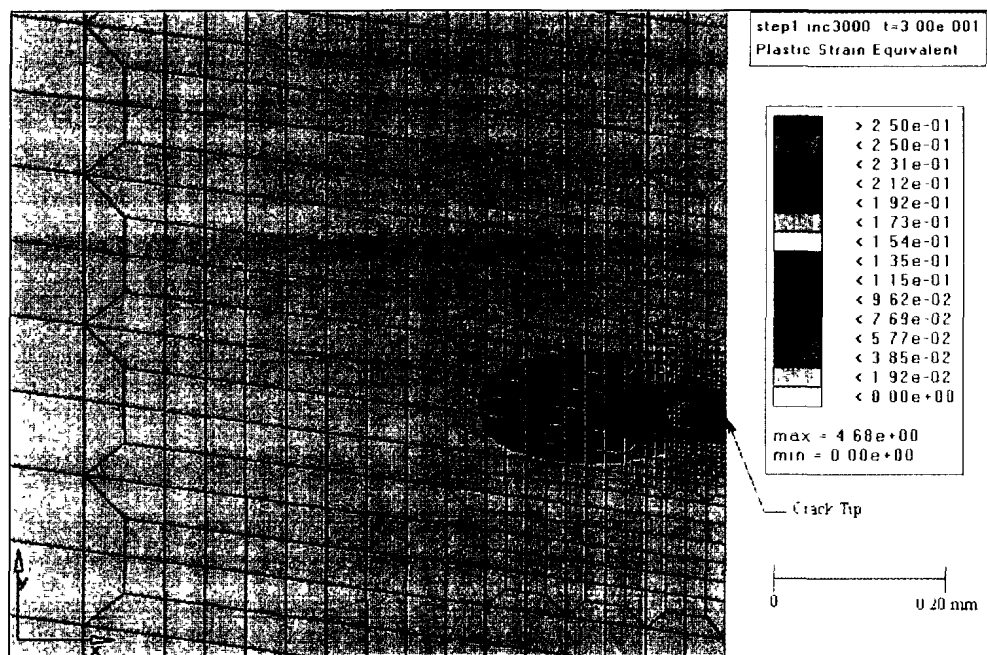


(c)

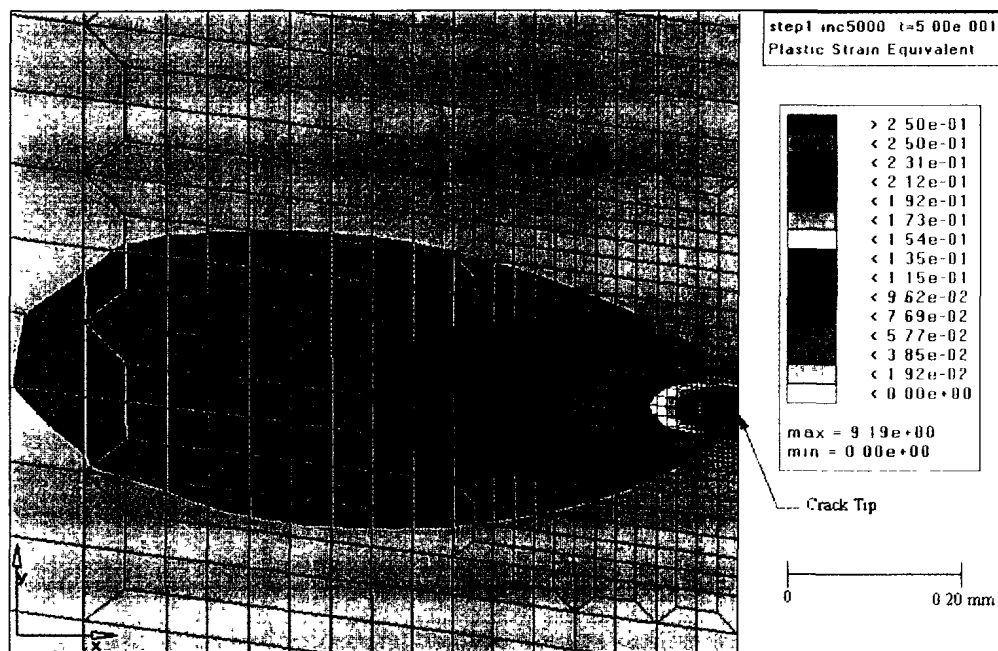


(d)

Figure 4.3 - Plastic Strain Contours in DT-304SS-08 Specimen  
(c)  $D_L/B = 0.02041$  (d)  $D_L/B = 0.02724$

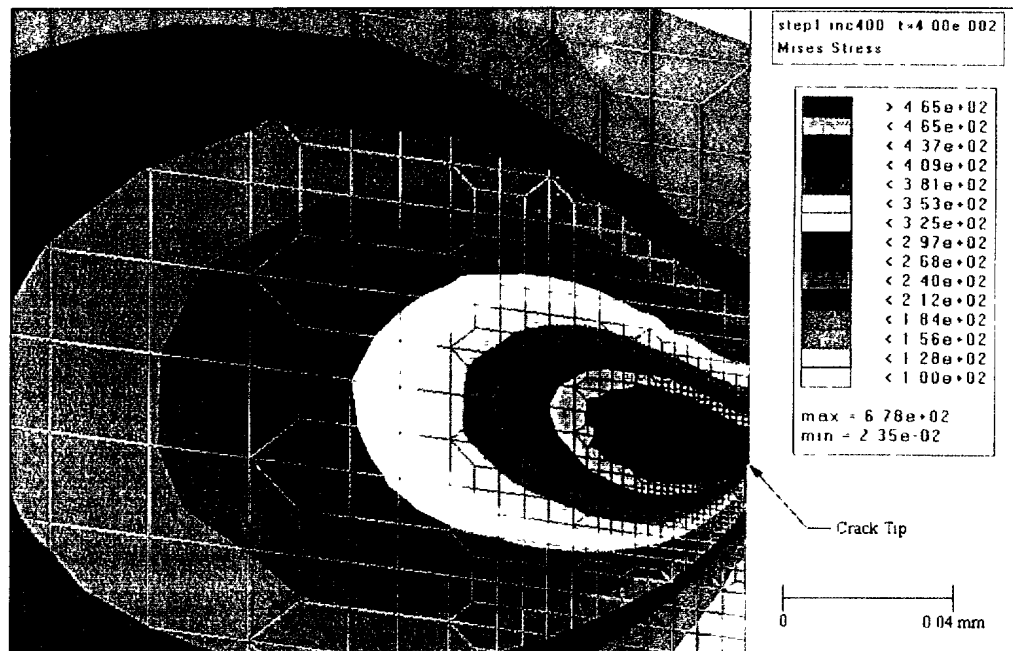


(e)

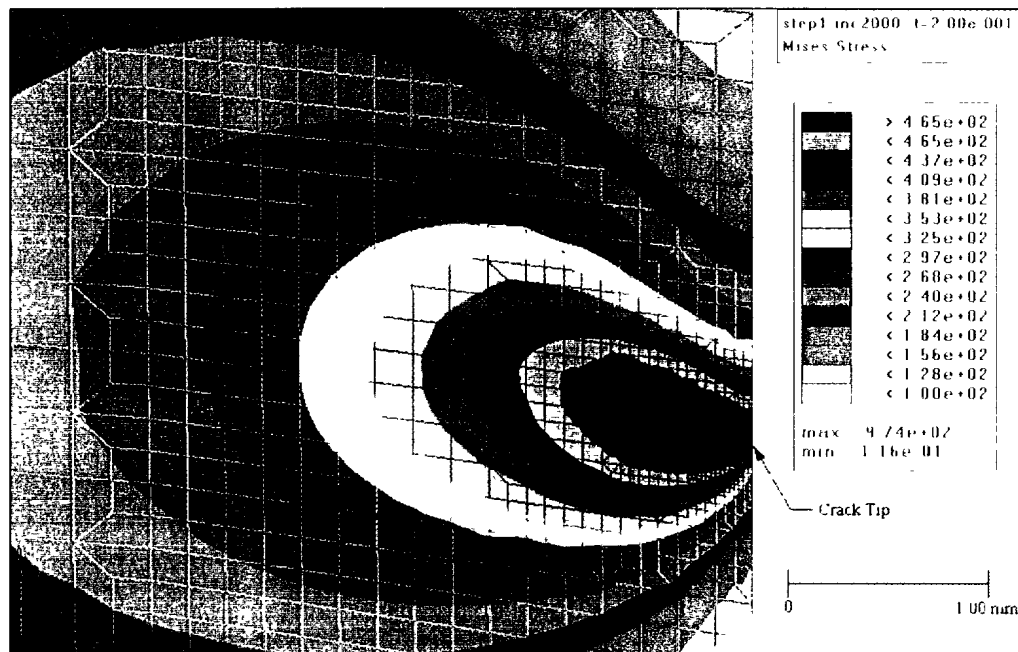


(f)

Figure 4.3 - Plastic Strain Contours in DT-304SS-08 Specimen  
(e)  $D_L / B = 0.04096$  (f)  $D_L / B = 0.06956$

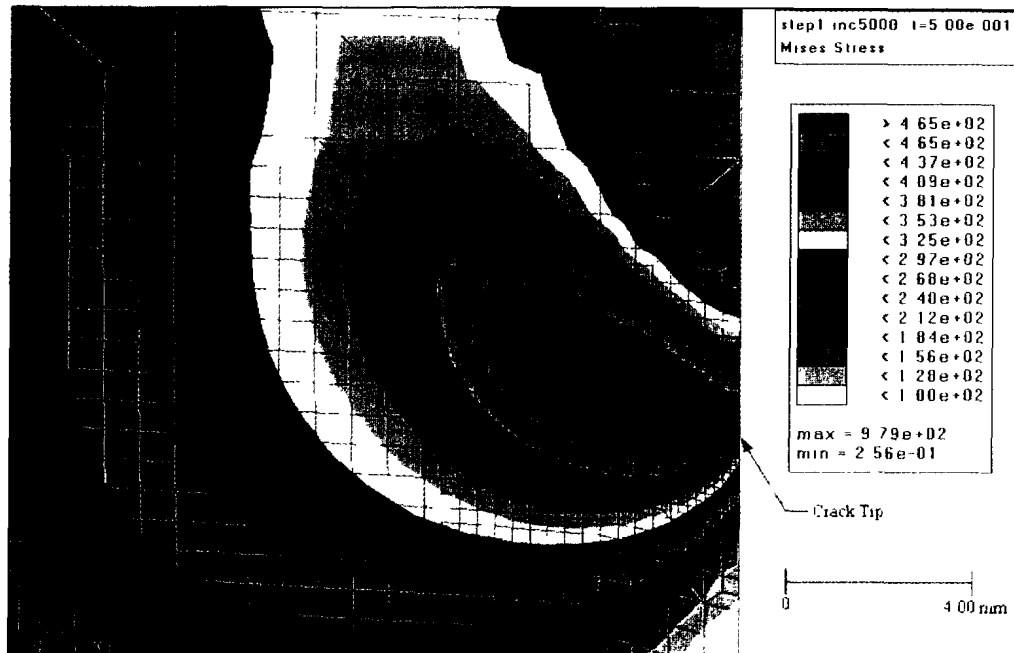


(a)



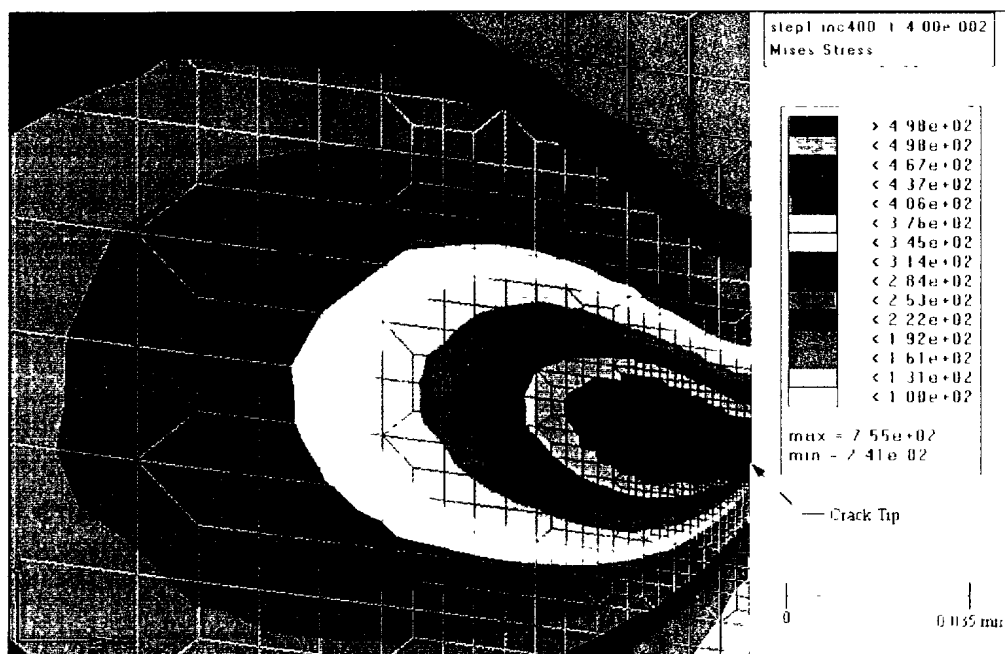
(b)

Figure 4.4: von Mises Stress Contours in DT-350WT-08 Specimen (a)  $D_L/B = 0.00544$  (b)  $D_L/B = 0.02724$

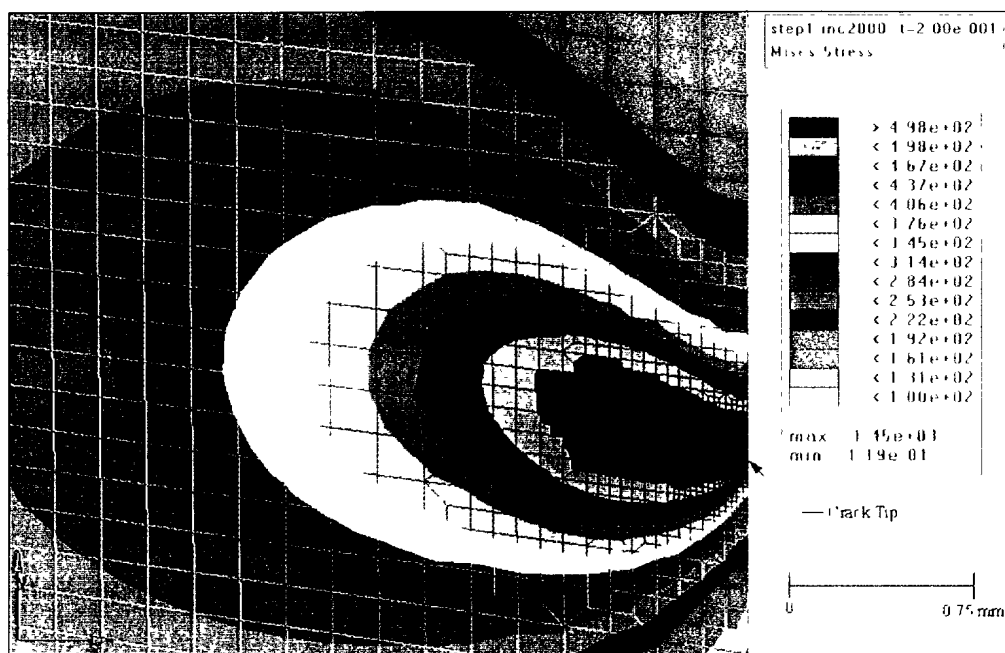


(c)

**Figure 4.4 - von Mises Stress Contours in DT-350WT-08 Specimen**  
**(c)  $D_L / B = 0.06964$**

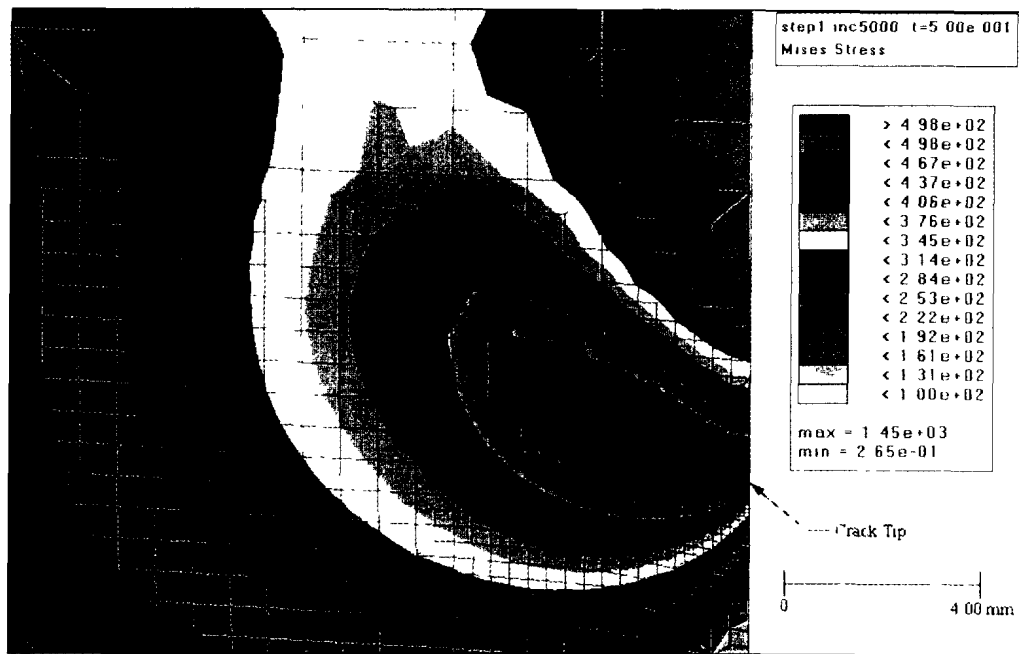


(a)



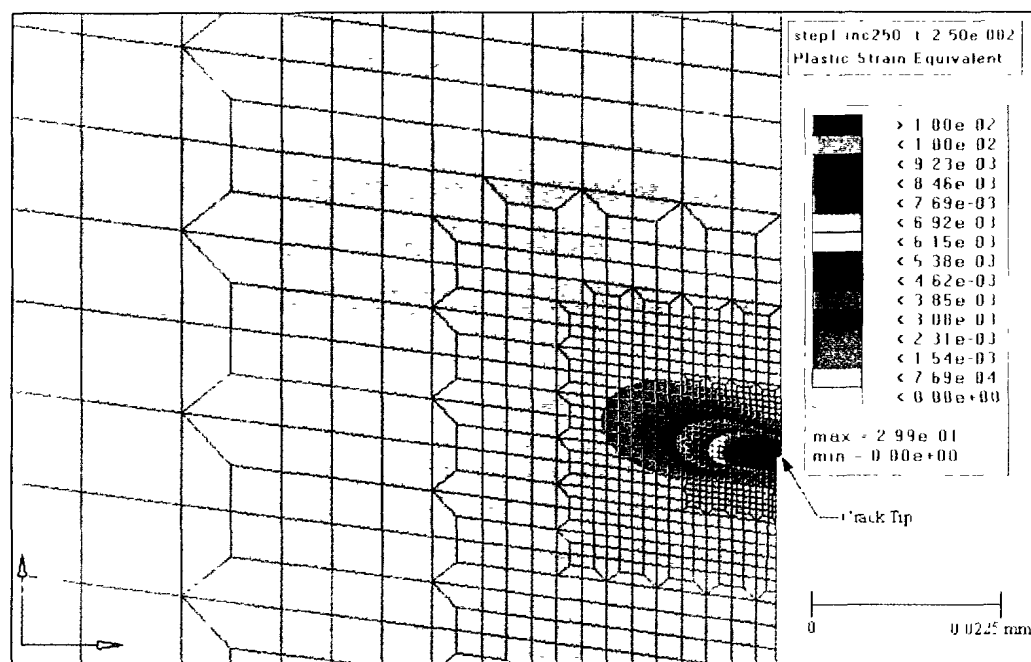
(b)

Figure 4.5: von Mises Stress Contours in DT-304SS-08 Specimen (a)  $D_L/B = 0.00544$  (b)  $D_L/B = 0.02724$

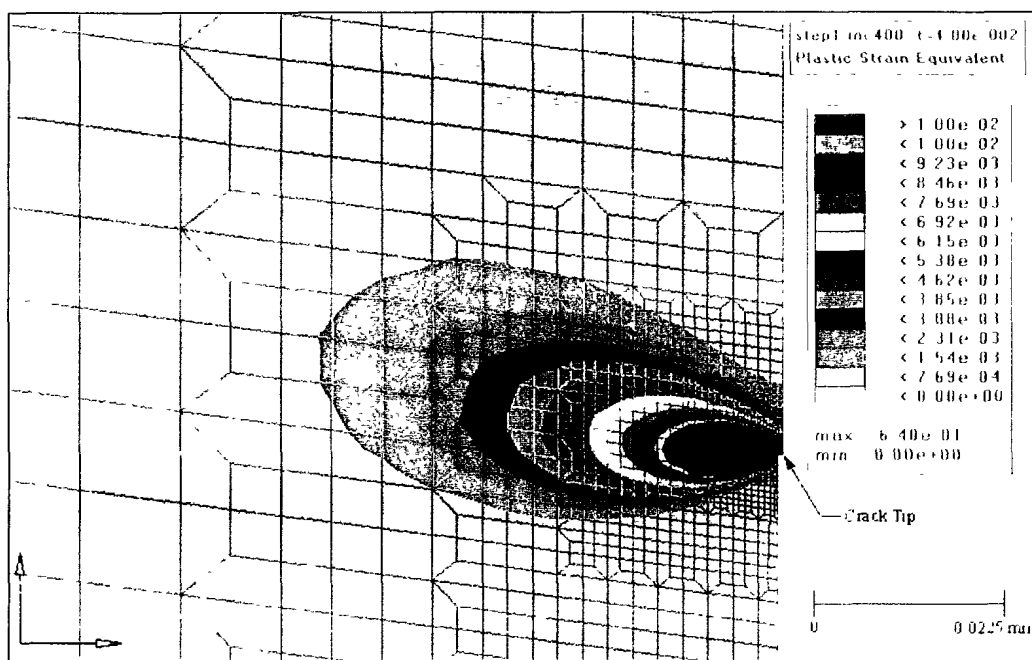


(c)

Figure 4.5: von Mises Stress Contours in DT-304SS-08 Specimen  
(c)  $D_L/B = 0.06956$

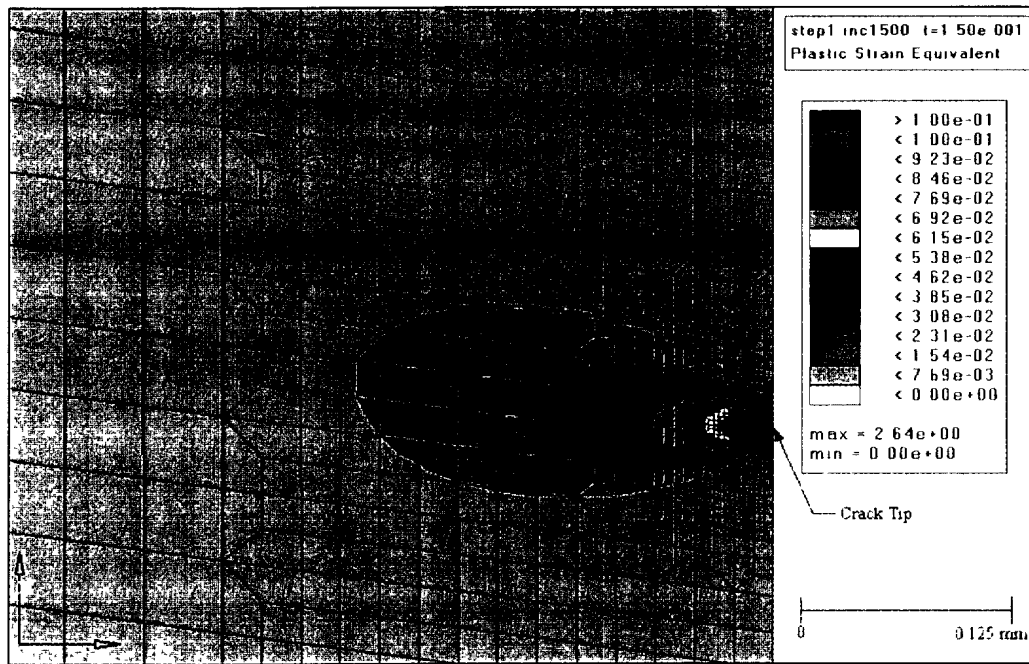


(a)

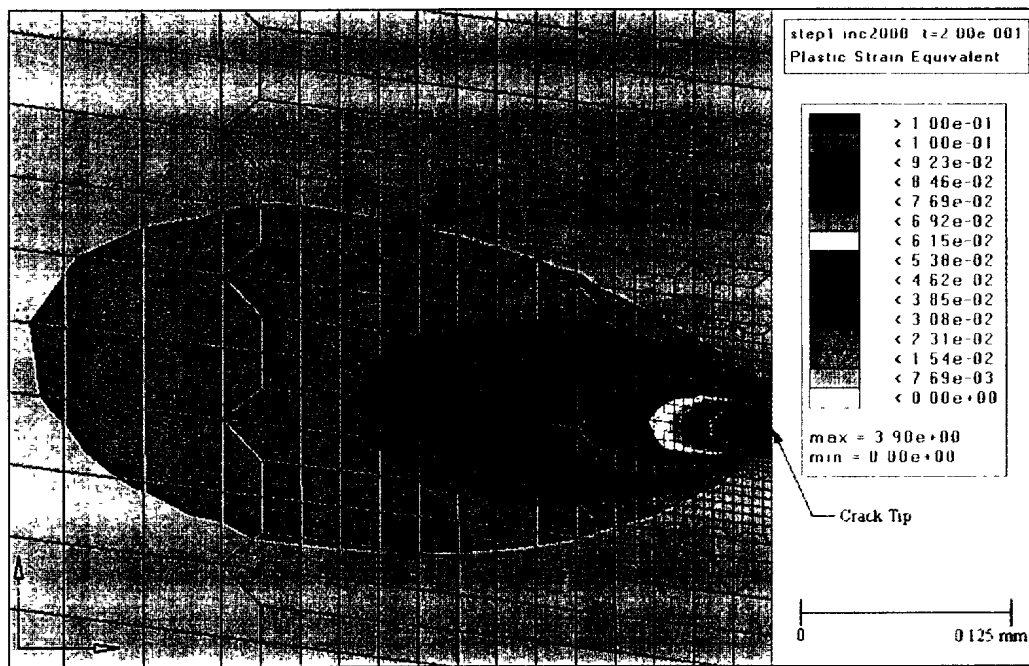


(b)

Figure 4.6: Plastic Strain Contours in NS-350WT-12 Specimen (a)  $D_L/B = 0.00250$  (b)  $D_L/B = 0.00401$



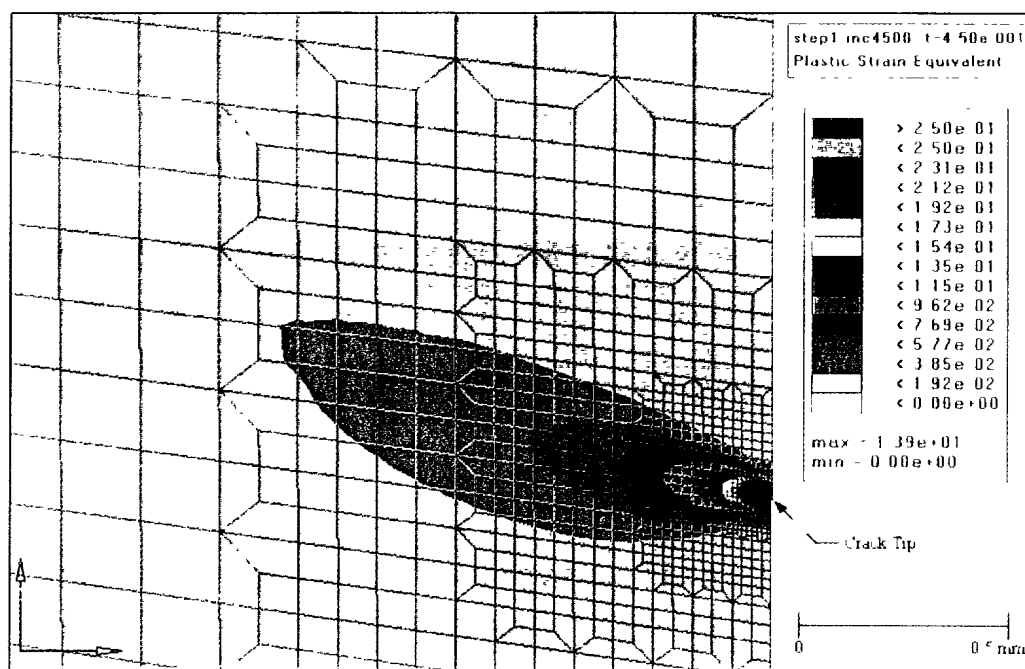
(c)



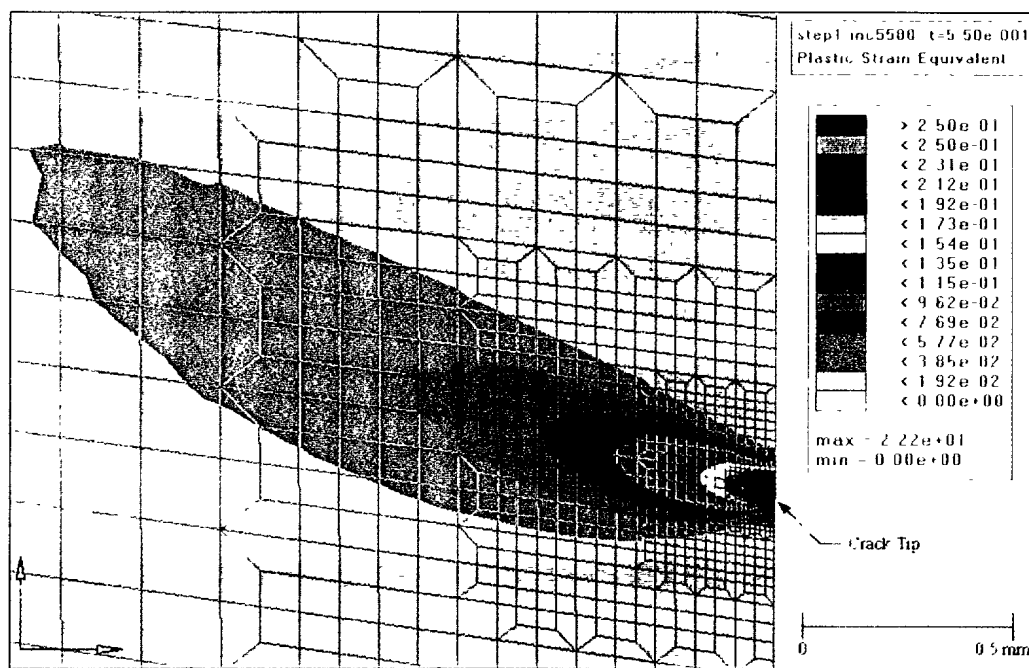
(d)

Figure 4.6: Plastic Strain Contours in NS-350WT-12 Specimen  
(c)  $D_L/B = 0.01497$  (d)  $D_L/B = 0.02001$



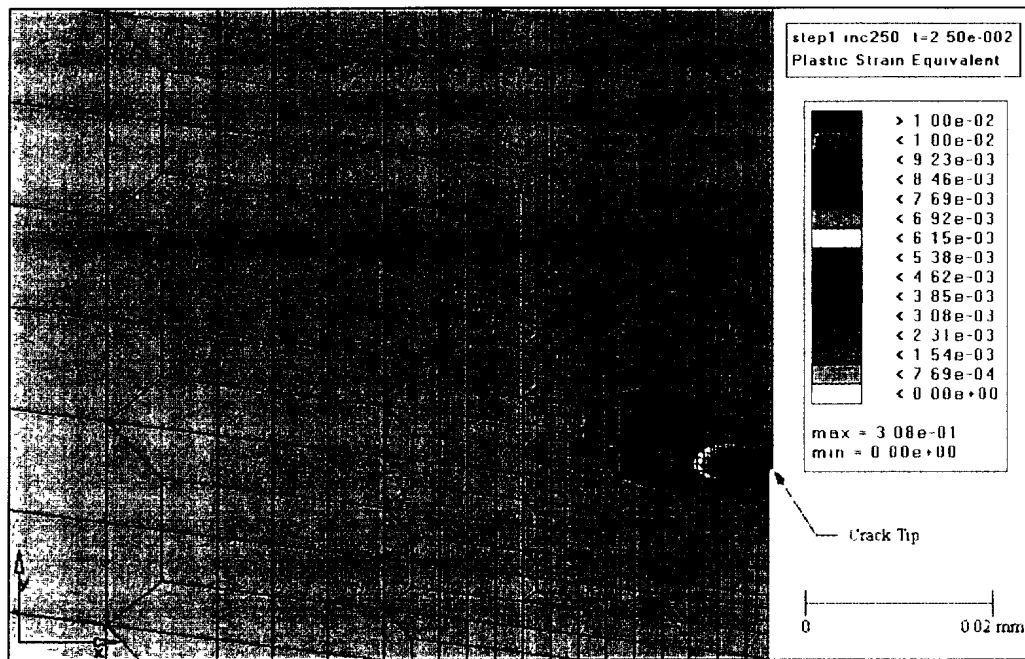


(e)

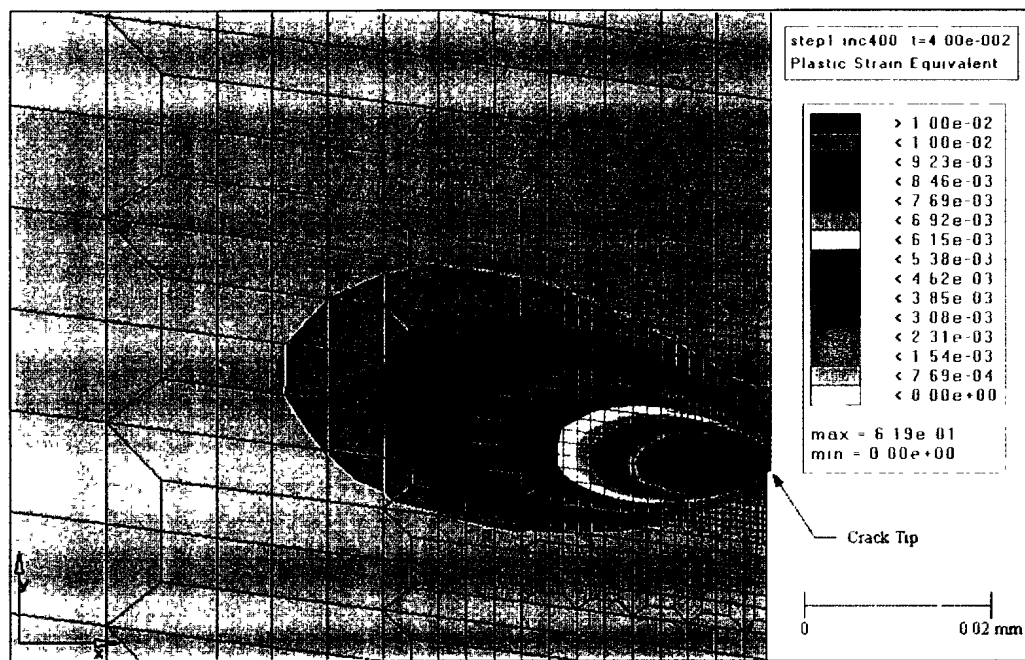


(f)

Figure 4.6: Plastic Strain Contours in NS-350WT-12 Specimen  
(e)  $D_L/B = 0.04490$  (f)  $D_L/B = 0.05477$

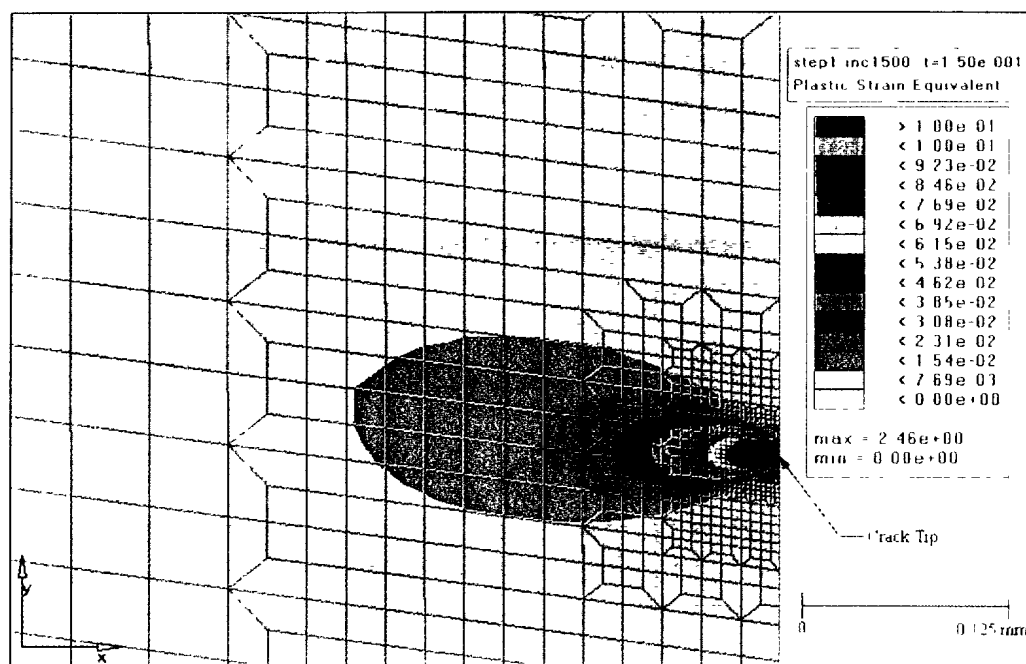


(a)

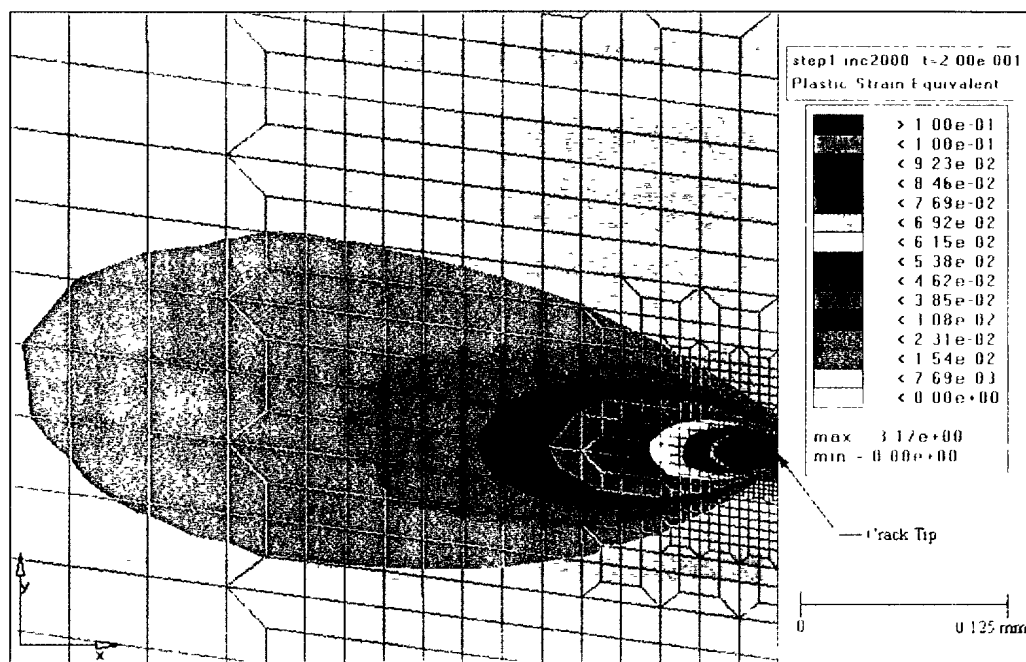


(b)

Figure 4.7: Plastic Strain Contours in NS-304SS-12 Specimen (a)  $D_L/B = 0.00250$  (b)  $D_L/B = 0.00421$

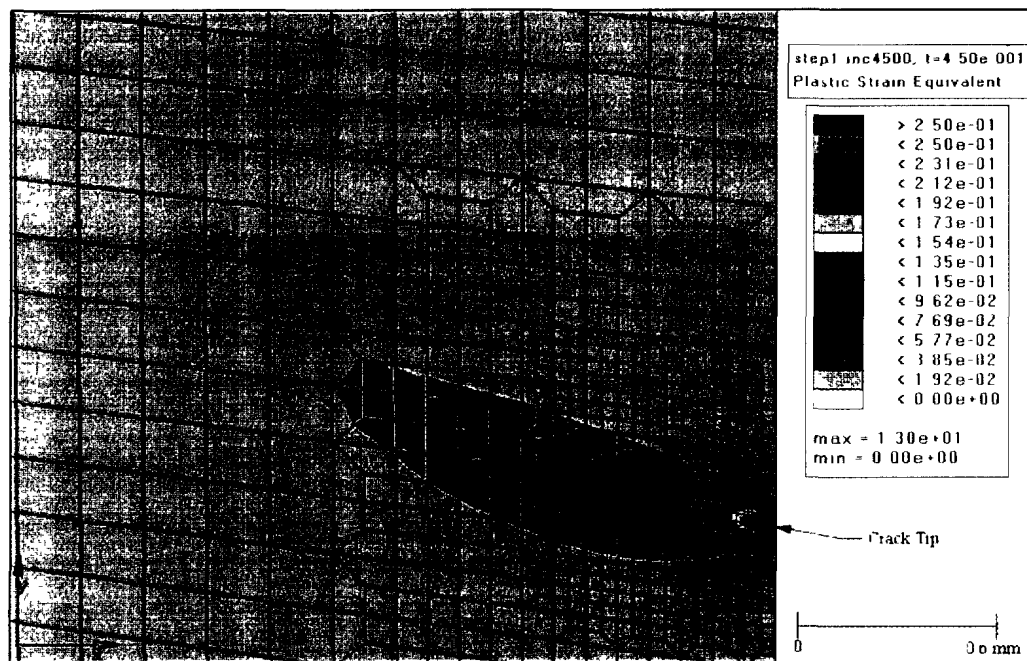


(c)

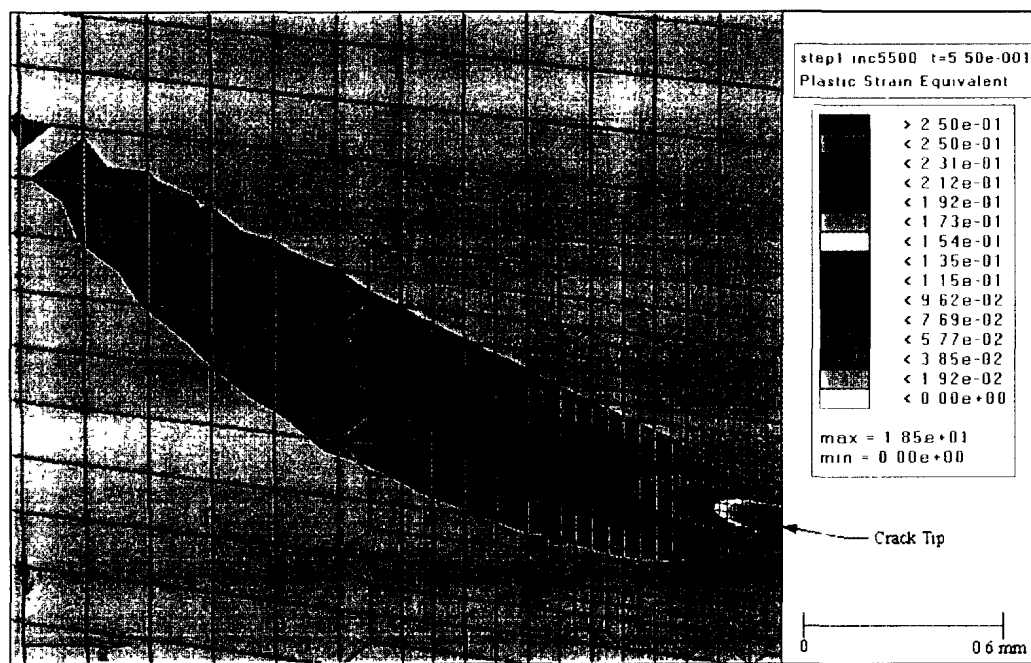


(d)

Figure 4.7: Plastic Strain Contours in NS-304SS-12 Specimen  
(c)  $D_L/B = 0.01513$  (d)  $D_L/B = 0.02022$

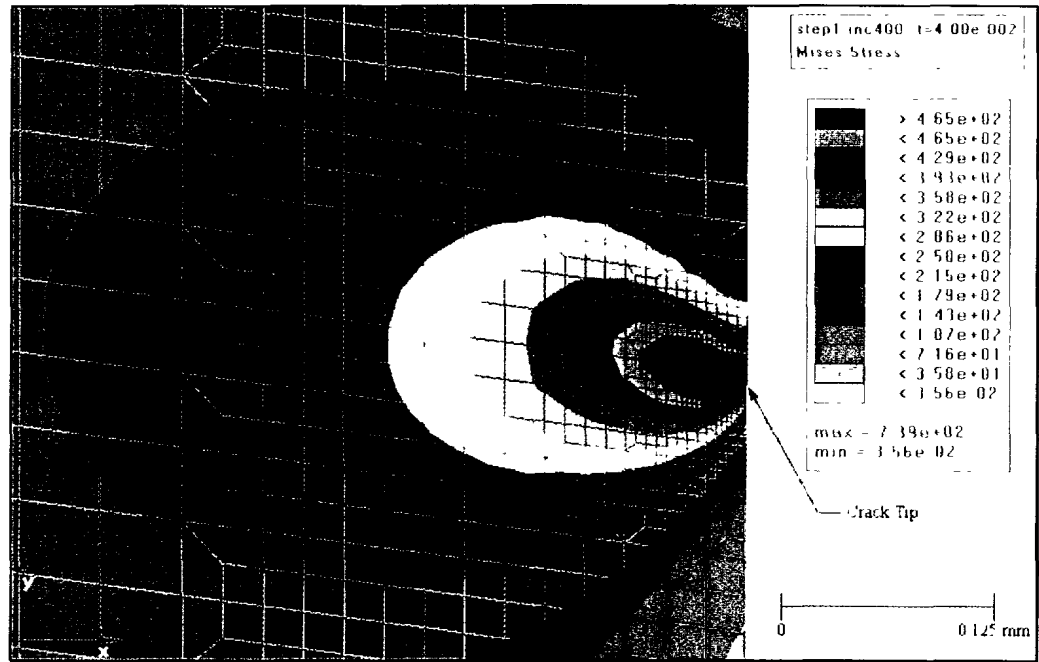


(e)

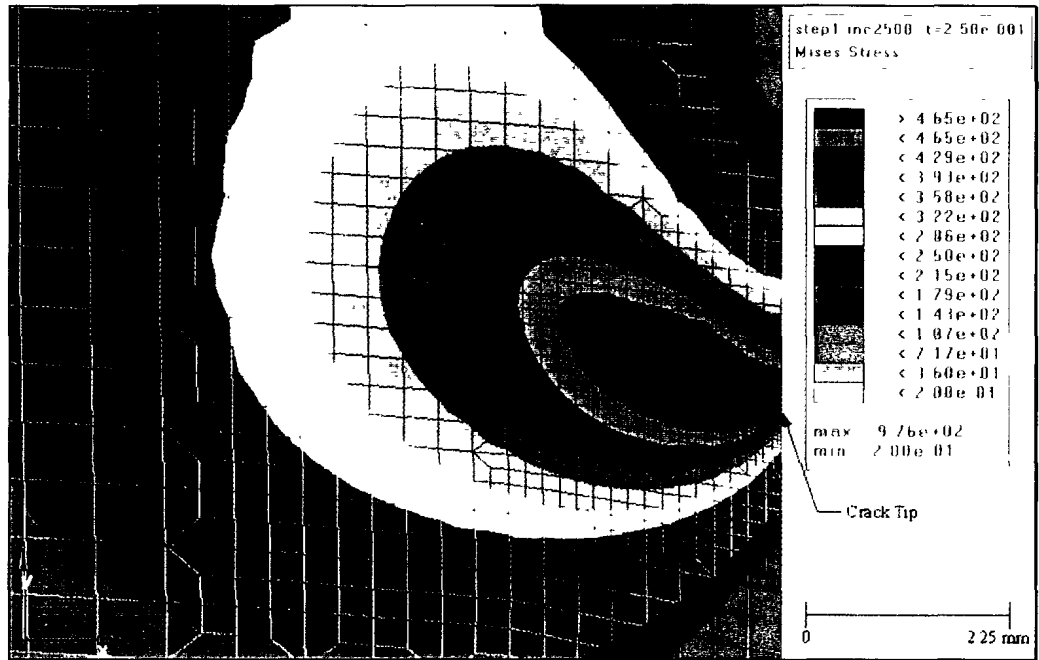


(f)

Figure 4.7: Plastic Strain Contours in NS-304SS-12 Specimen  
(e)  $D_L/B = 0.04564$  (f)  $D_L/B = 0.04928$



(a)



(b)

Figure 4.8: von Mises Stress Contours in NS-350WT-12 Specimen (a) $D_L/B = 0.00401$  (b) $D_L/B = 0.02505$

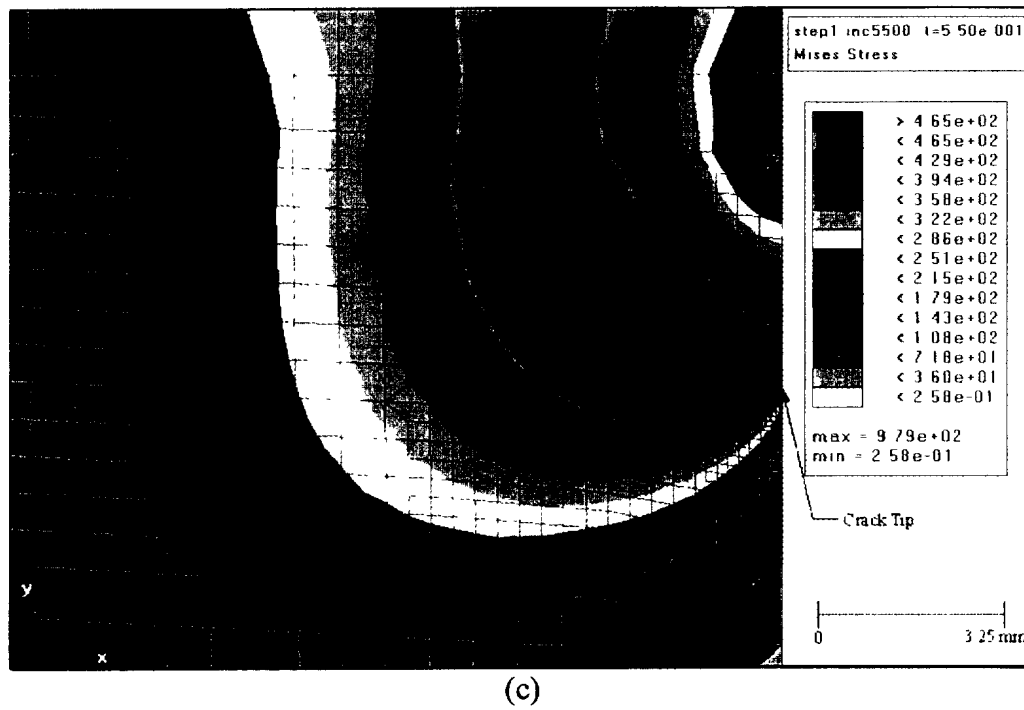
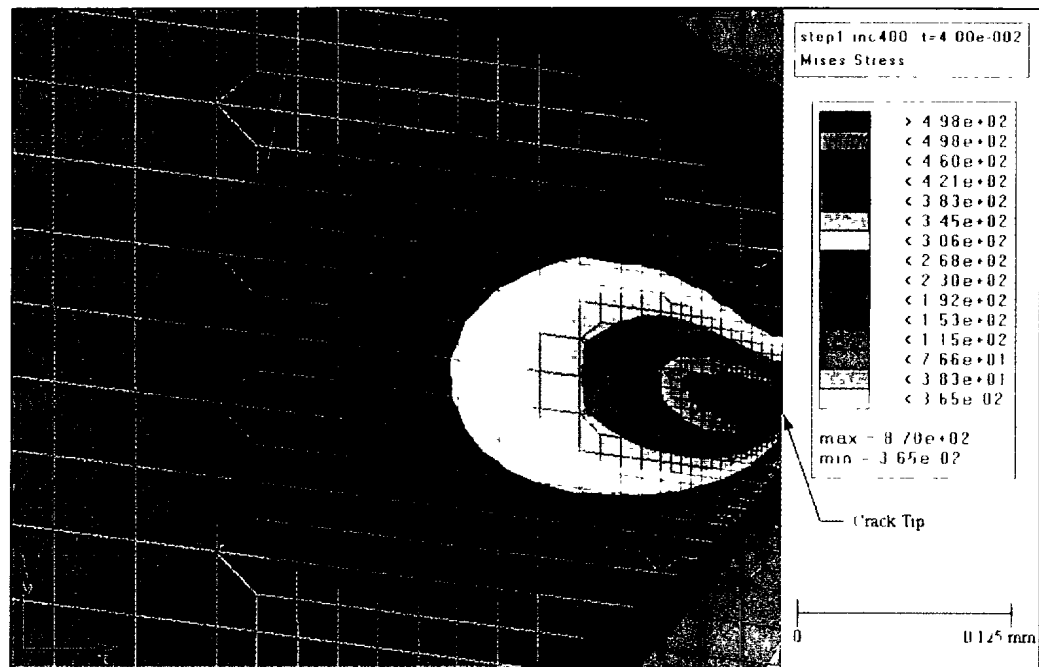
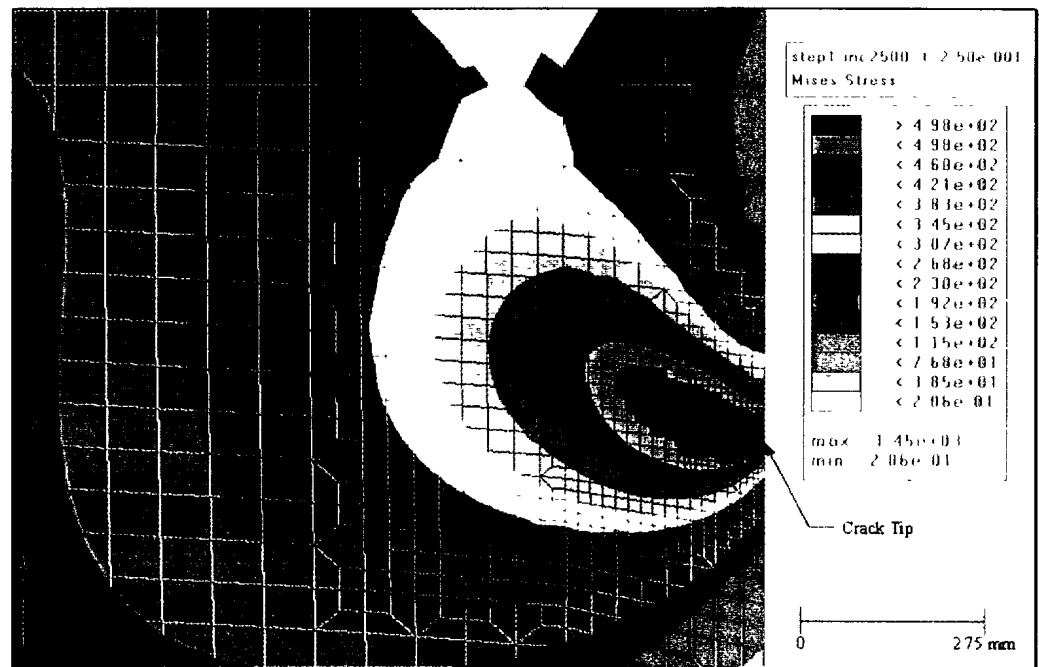


Figure 4.8: von Mises Stress Contours in NS-350WT-12 Specimen  
(a)  $D_L/B = 0.05477$



(a)



(b)

Figure 4.9: von Mises Stress Contours in NS-304SS-12 Specimen (a)  $D_L/B = 0.00421$  (b)  $D_L/B = 0.02532$

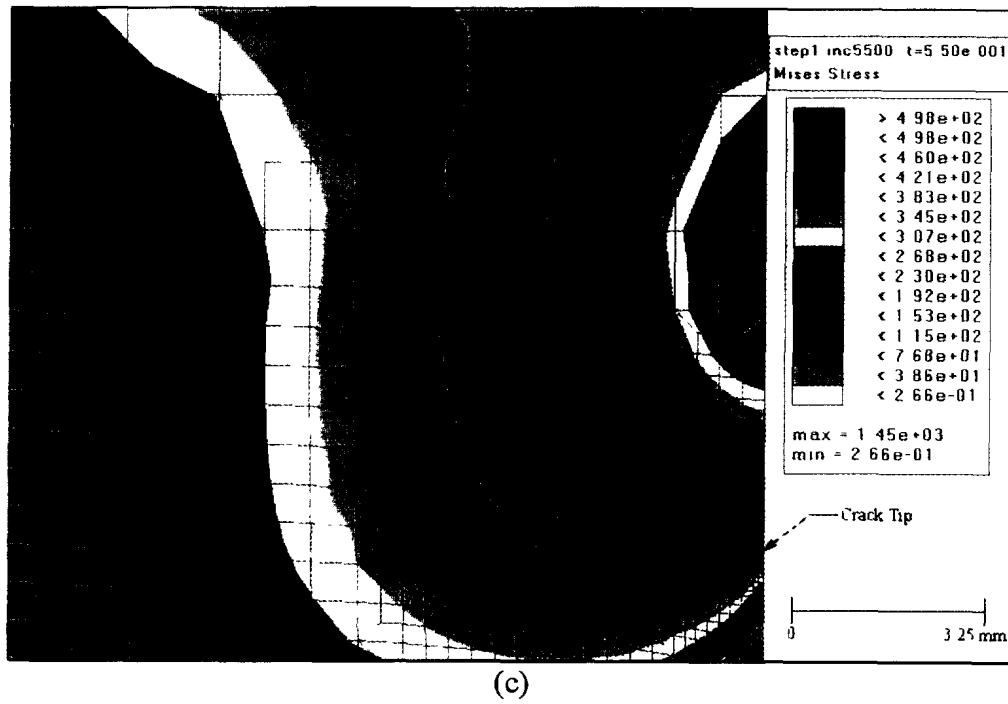
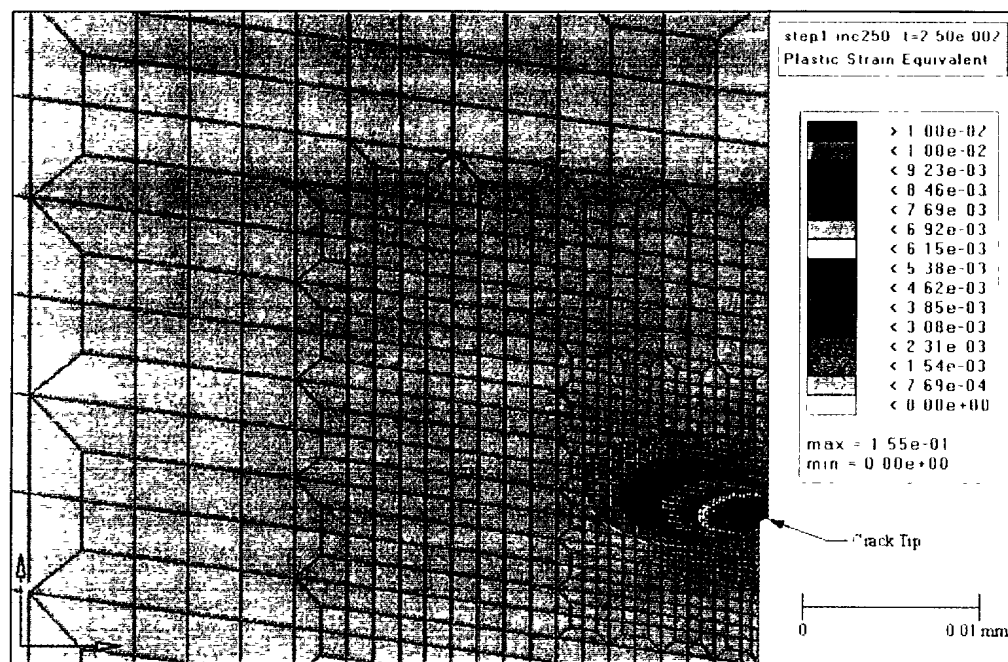
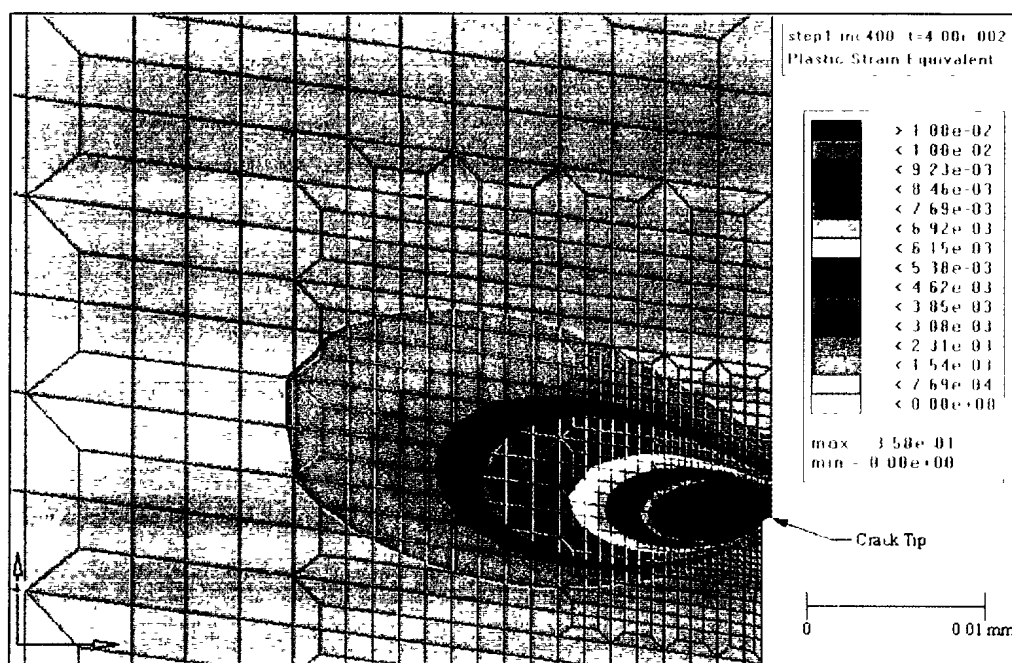


Figure 4.9: von Mises Stress Contours in NS-304SS-12 Specimen  
(c)  $D_L/B = 0.04928$



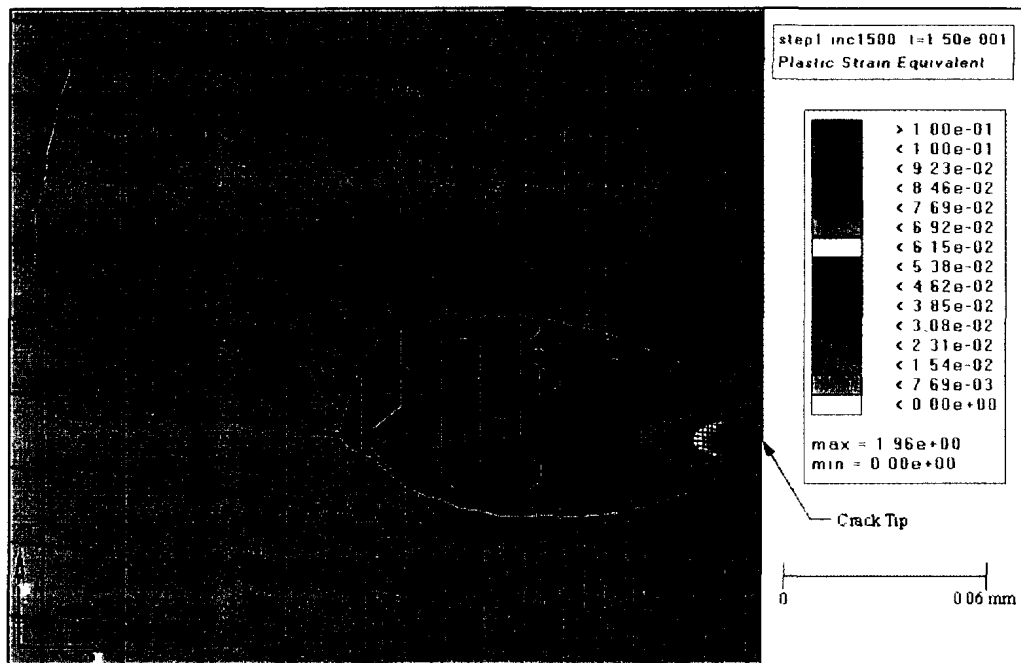


(a)

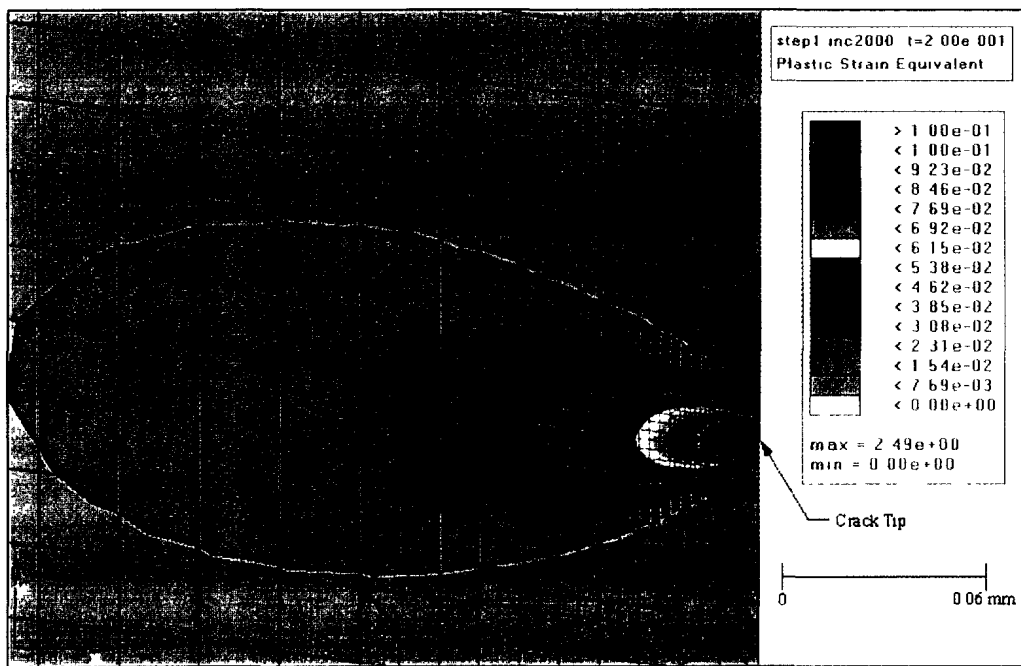


(b)

Figure 4.10: Plastic Strain Contours in DT-350WT-25 Specimen (a)  $D_L/B = 0.00111$  (b)  $D_L/B = 0.00178$

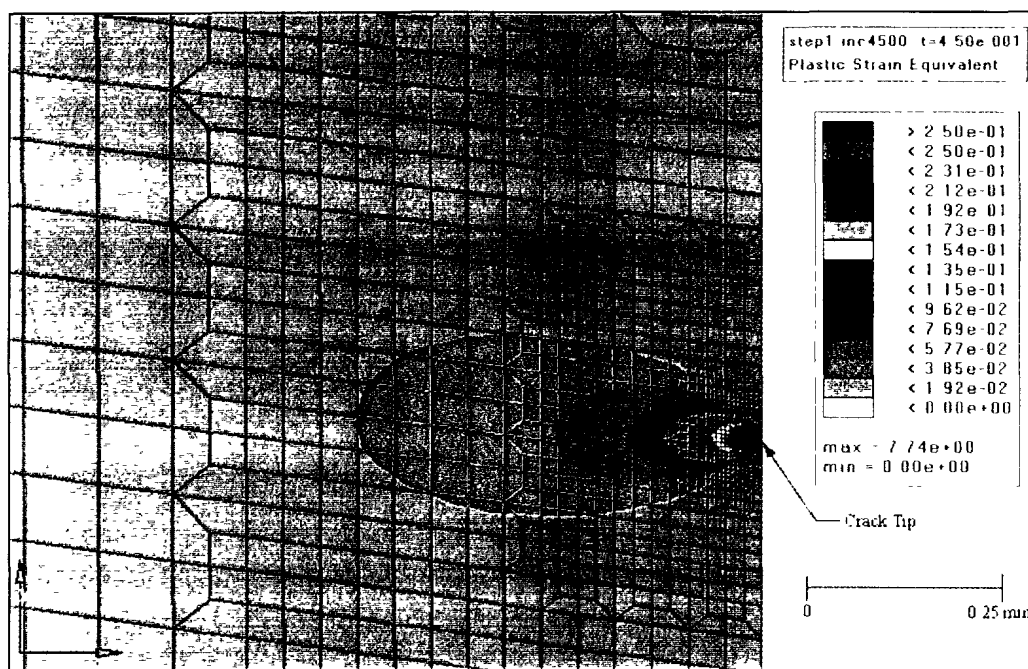


(c)

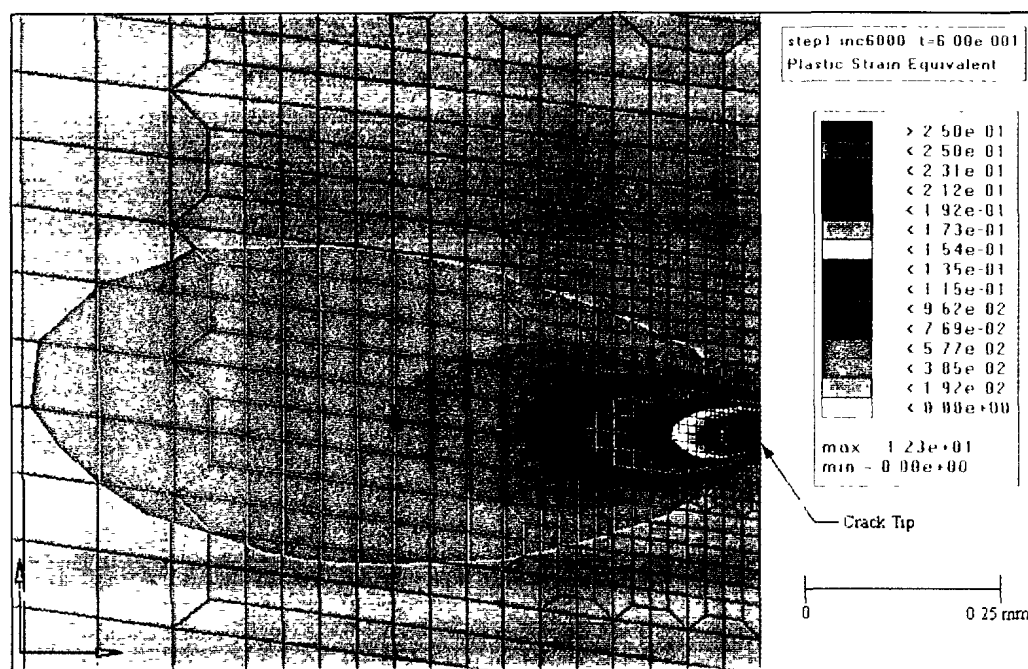


(d)

Figure 4.10: Plastic Strain Contours in DT-350WT-25 Specimen  
(c)  $D_L/B = 0.00667$  (d)  $D_L/B = 0.00890$

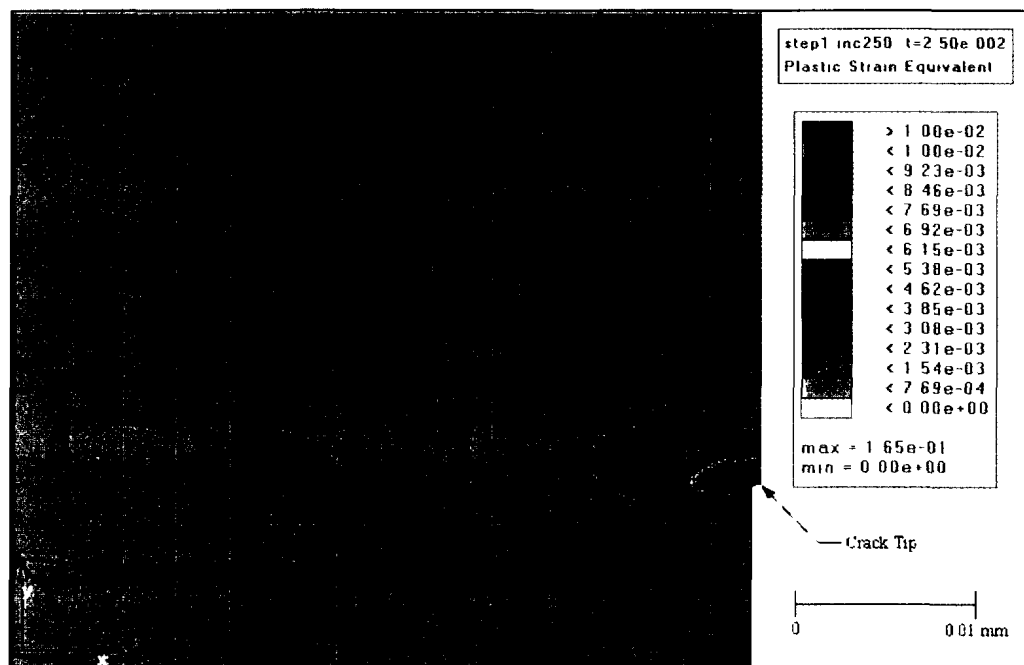


(e)

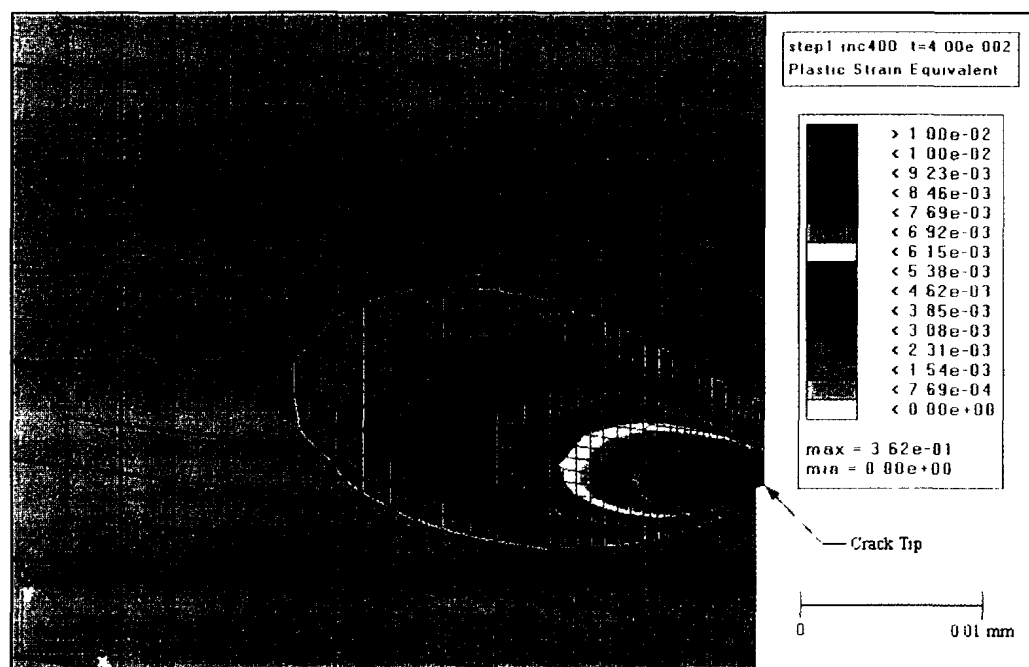


(f)

Figure 4.10: Plastic Strain Contours in DT-350WT-25 Specimen  
(e)  $D_L/B = 0.02027$  (f)  $D_L/B = 0.02754$

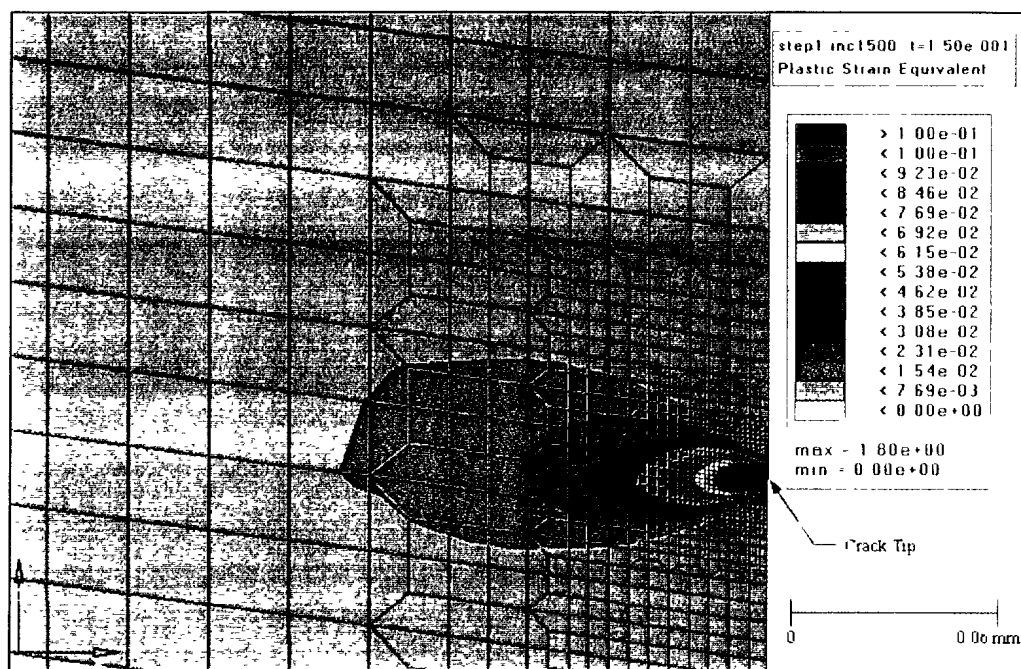


(a)

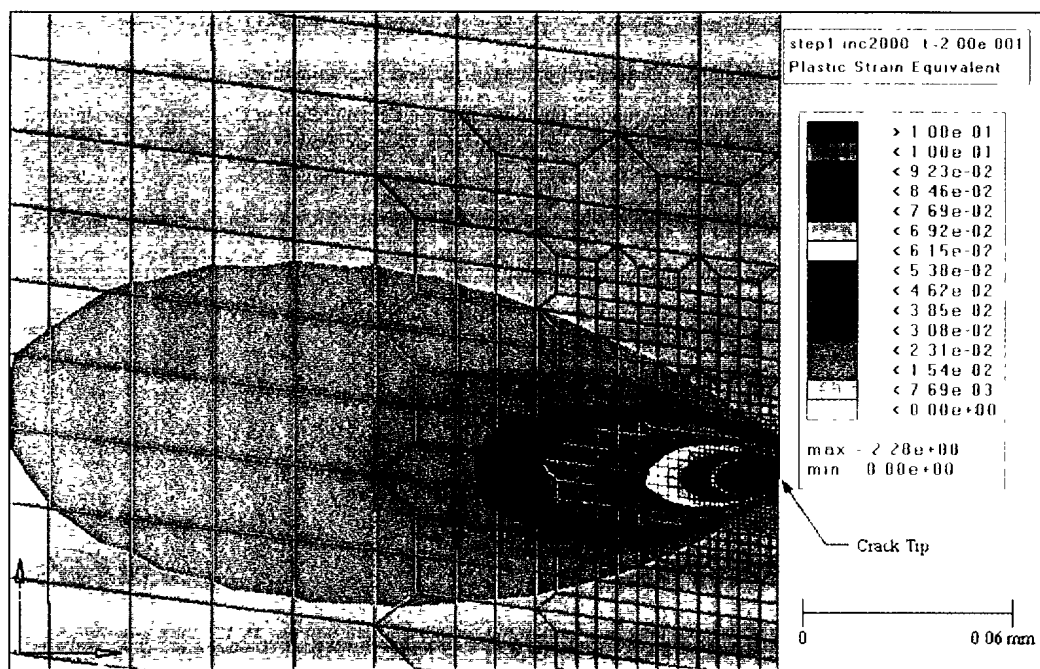


(b)

Figure 4.11: Plastic Strain Contours in DT-304SS-25 Specimen (a)  $D_L/B = 0.00111$  (b)  $D_L/B = 0.00178$

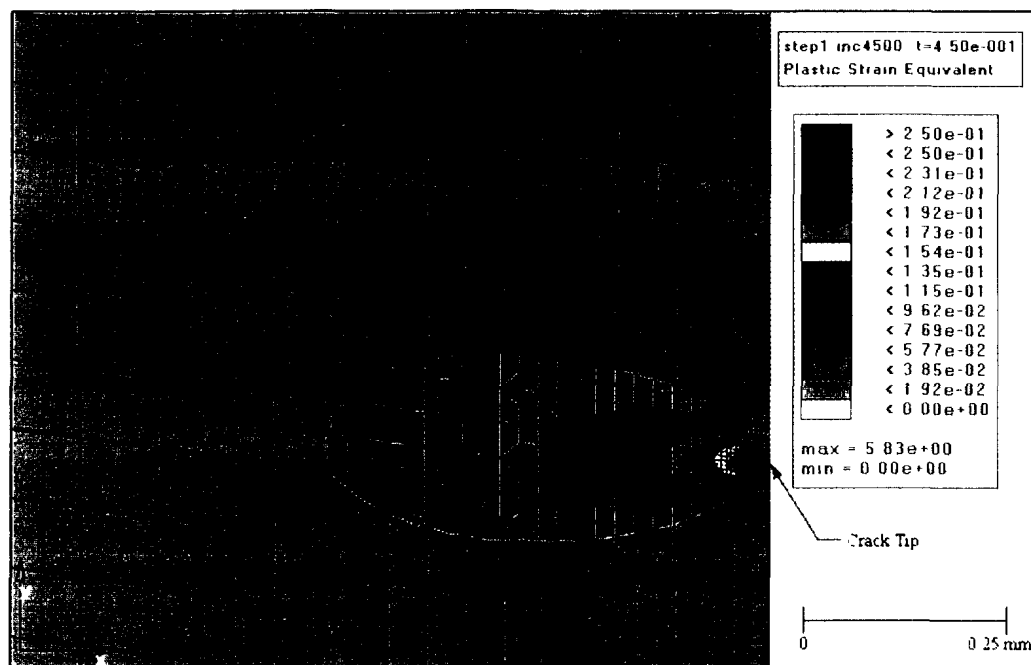


(c)

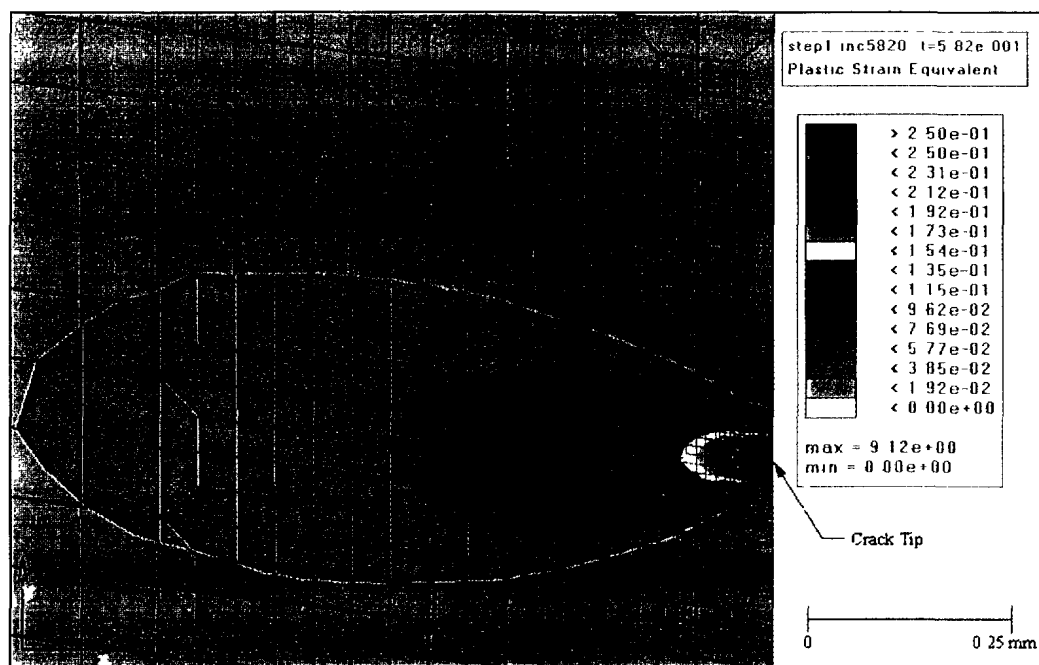


(d)

Figure 4.11: Plastic Strain Contours in DT-304SS-25 Specimen  
(c)  $D_L/B = 0.00667$  (d)  $D_L/B = 0.00889$

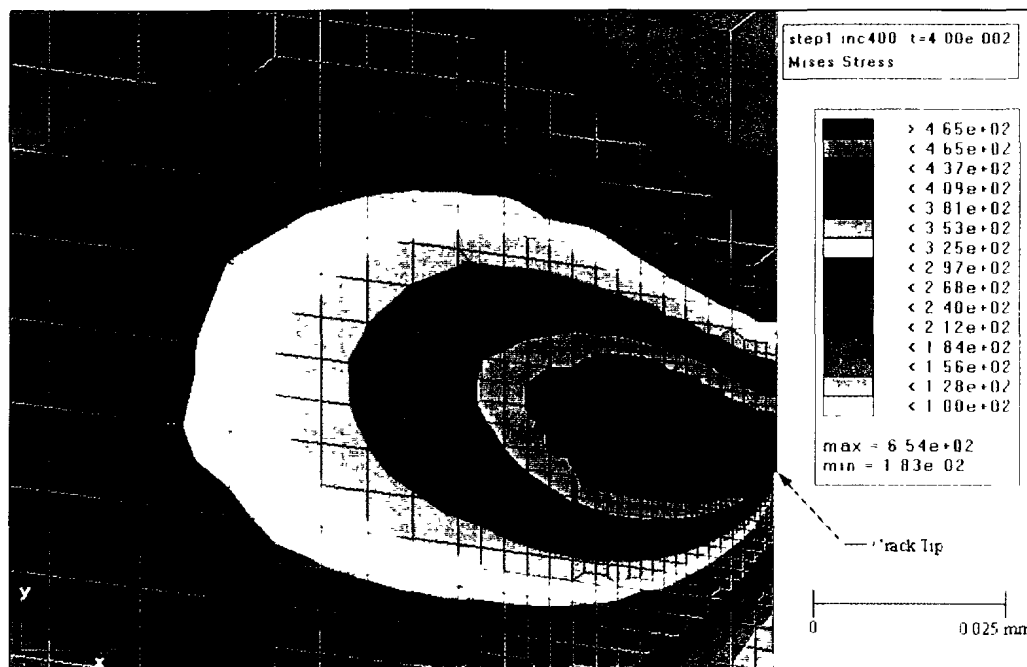


(e)

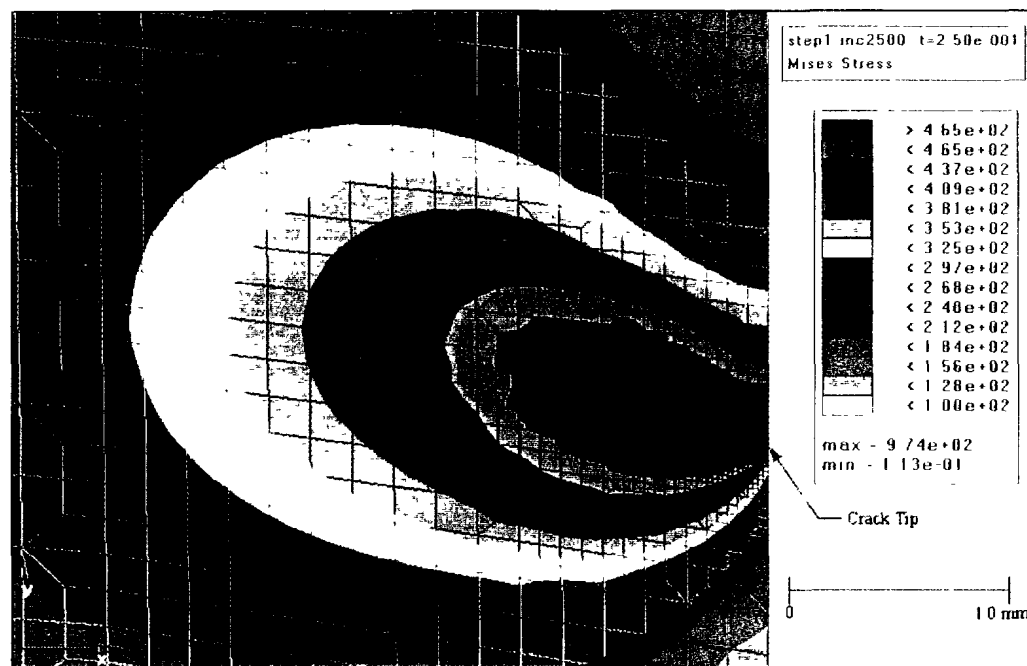


(f)

Figure 4.11: Plastic Strain Contours in DT-304SS-25 Specimen  
(e)  $D_L/B = 0.02024$  (f)  $D_L/B = 0.02660$



(a)



(b)

Figure 4.12: von Mises Stress Contours in DT-350WT-25 Specimen (a)  $D_L/B = 0.00178$  (b)  $D_L/B = 0.01113$

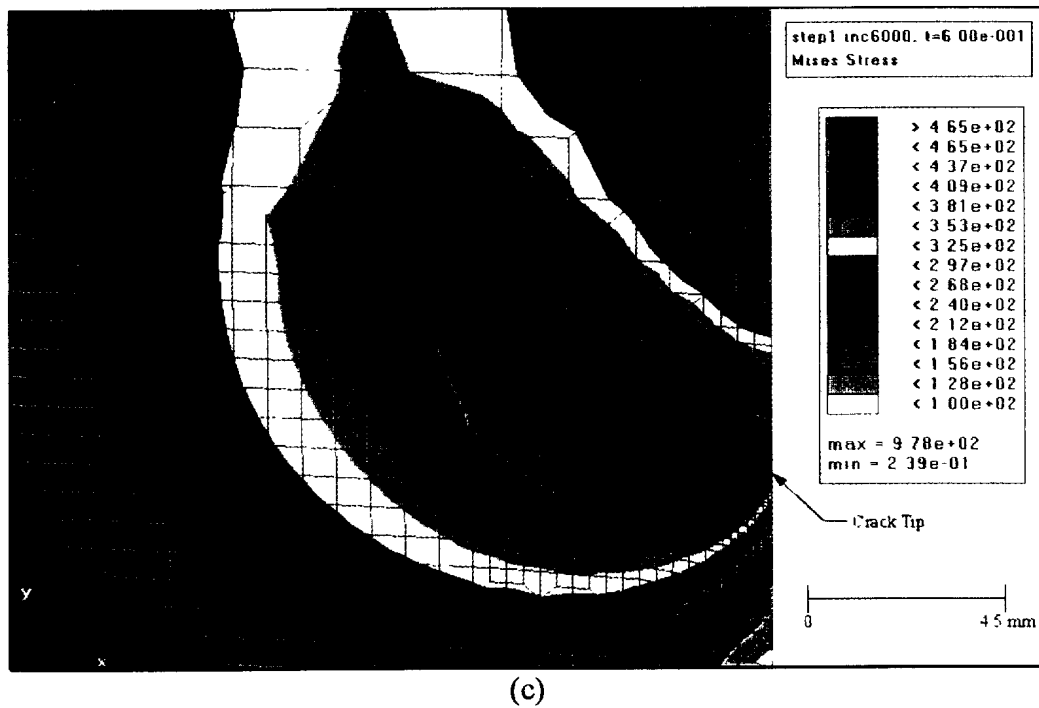
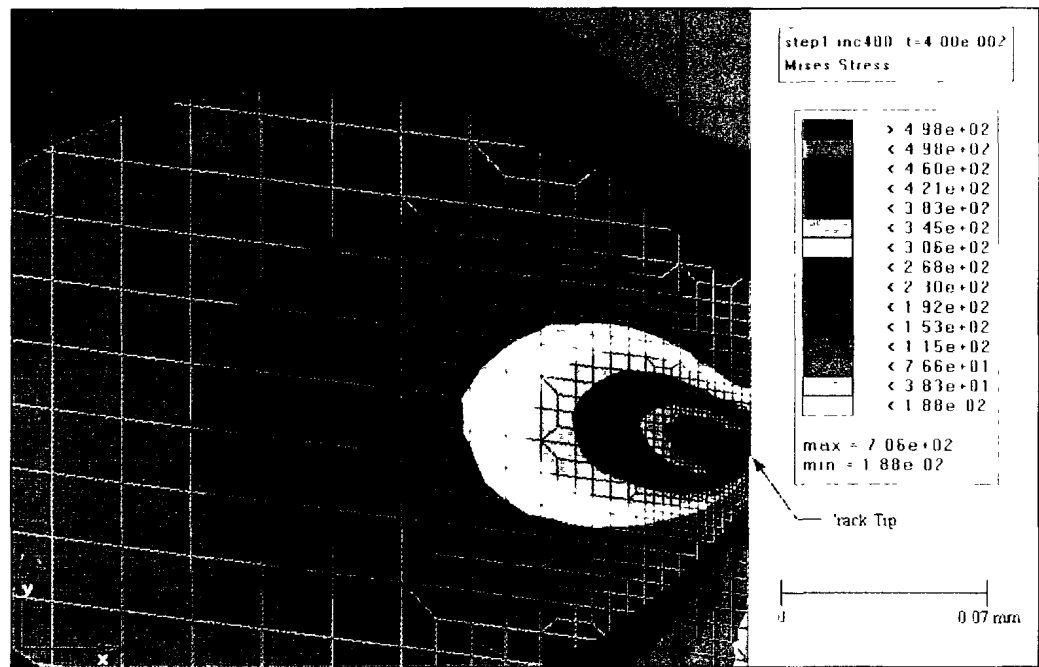
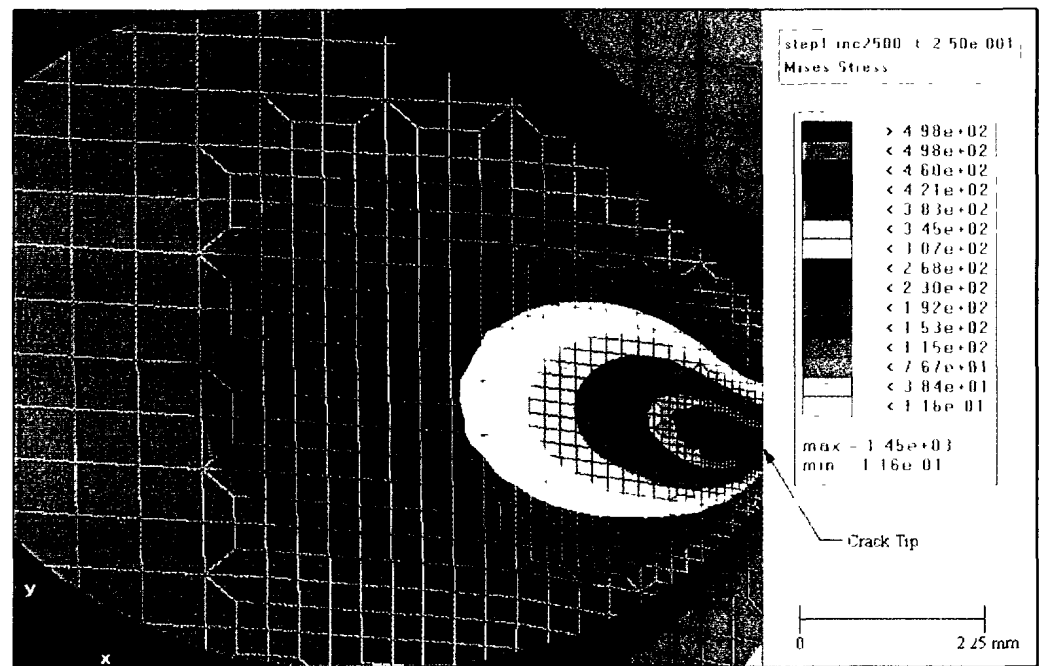


Figure 4.12: von Mises Stress Contours in DT-350WT-25 Specimen  
(c)  $D_L/B = 0.02754$



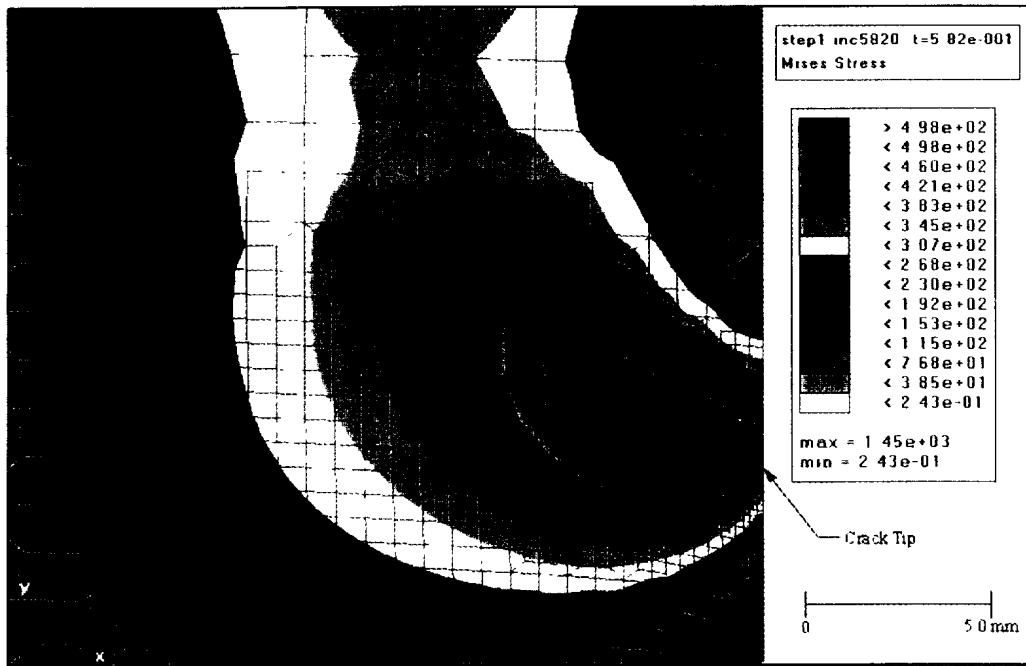


(a)



(b)

Figure 4.13: von Mises Stress Contours in DT-304SS-25 Specimen (a)  $D_L/B = 0.00178$  (b)  $D_L/B = 0.01113$



(c)

Figure 4.13: von Mises Stress Contours in DT-304SS-25 Specimen  
(c)  $D_L/B = 0.02660$

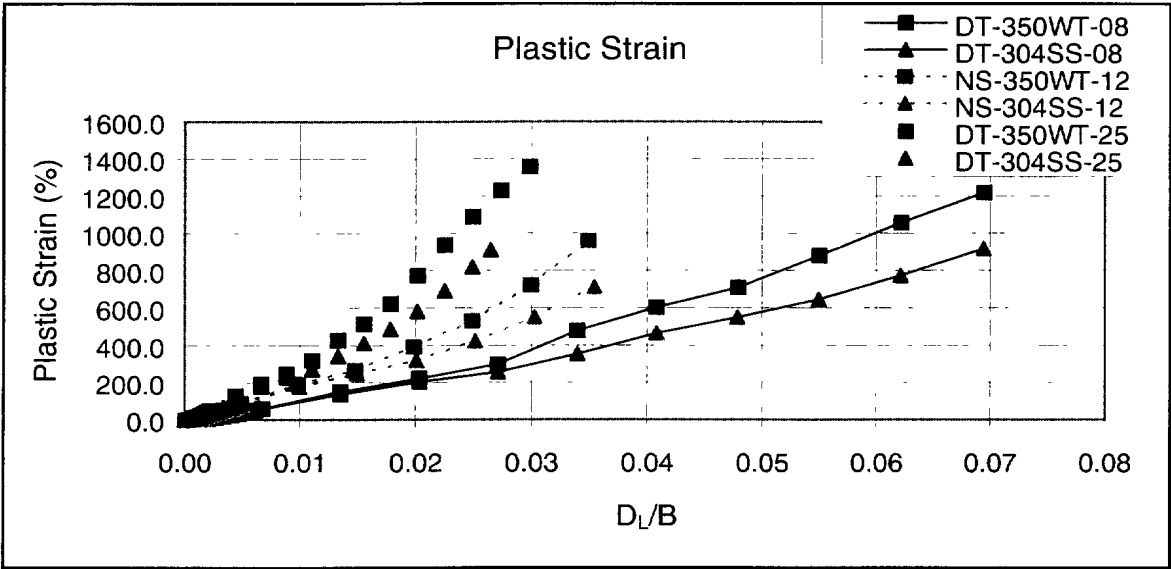


Figure 4.14: Variation of Maximum Plastic Strain with Non-Dimensionalized Displacement for all Specimens

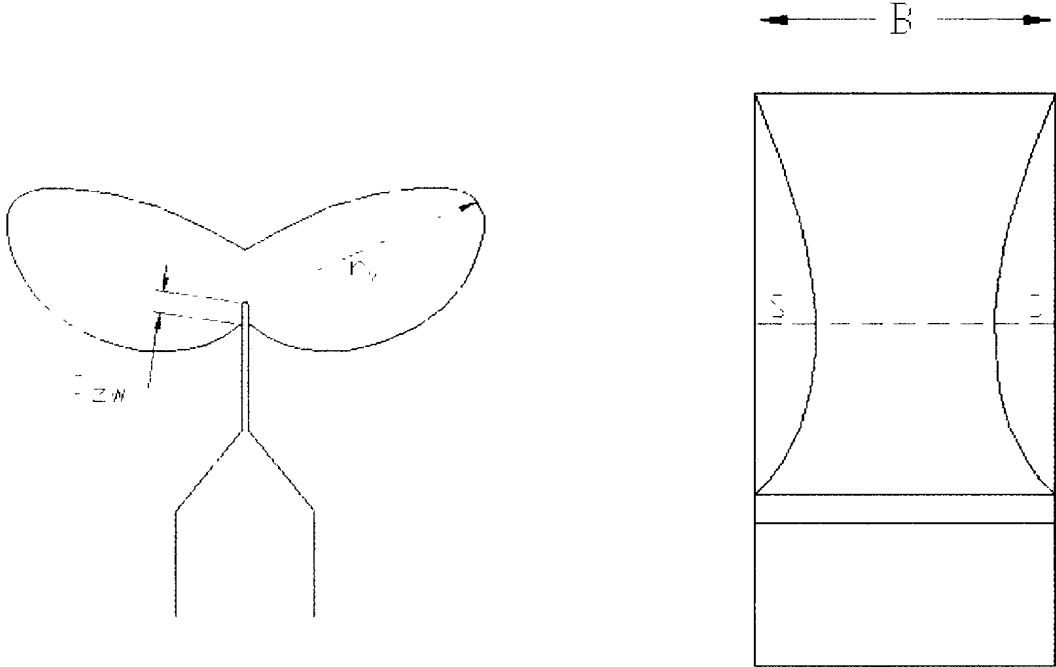


Figure 4.15: Schematic Illustration of Plastic Radius ( $r_y$ ) and Stretch Zone Width (SZW)

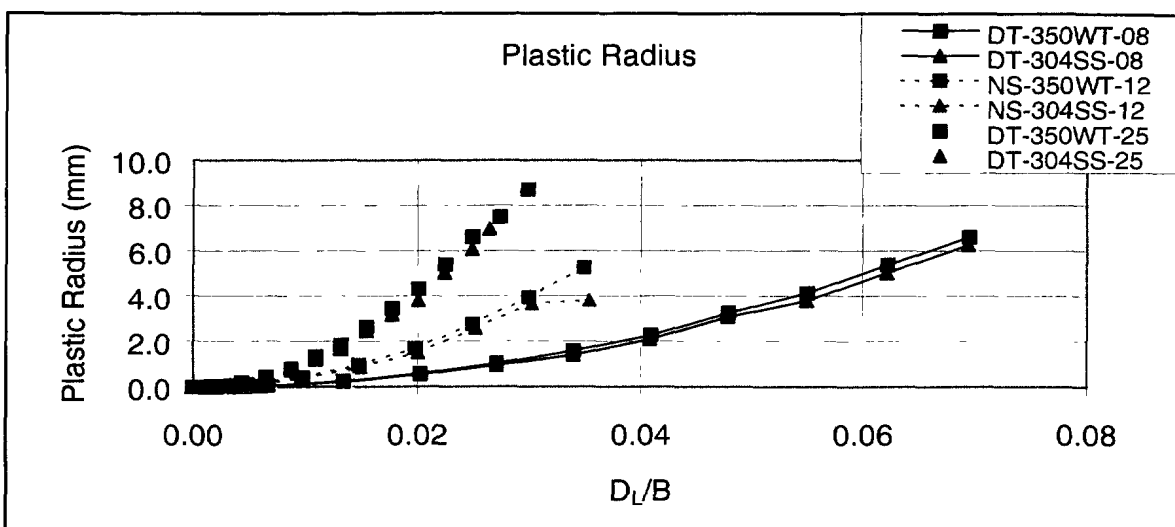


Figure 4.16: Variation of Plastic Radius with Non-Dimensionalized Displacement for all Specimens

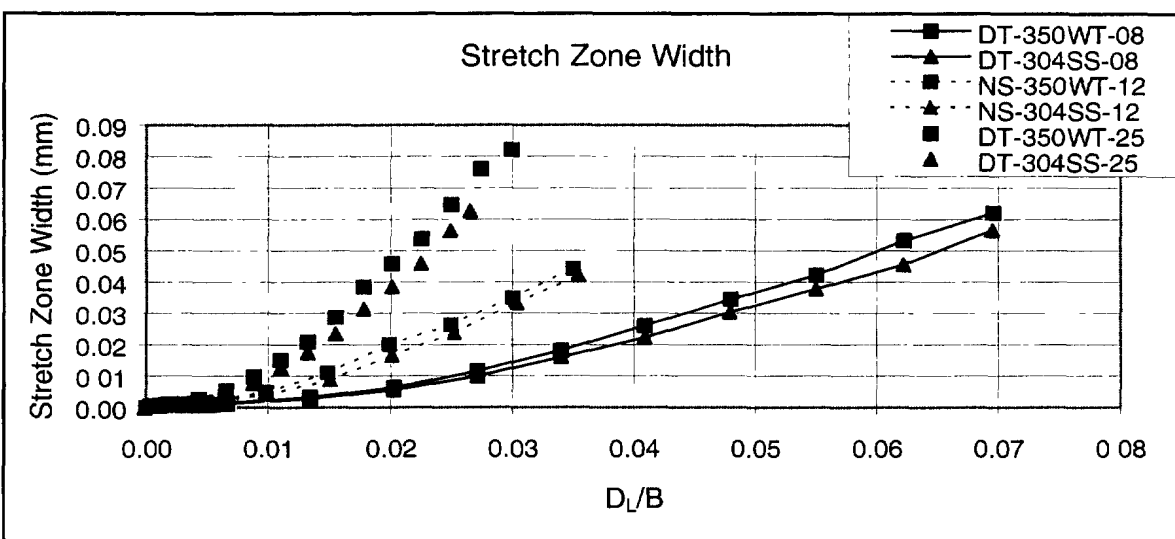
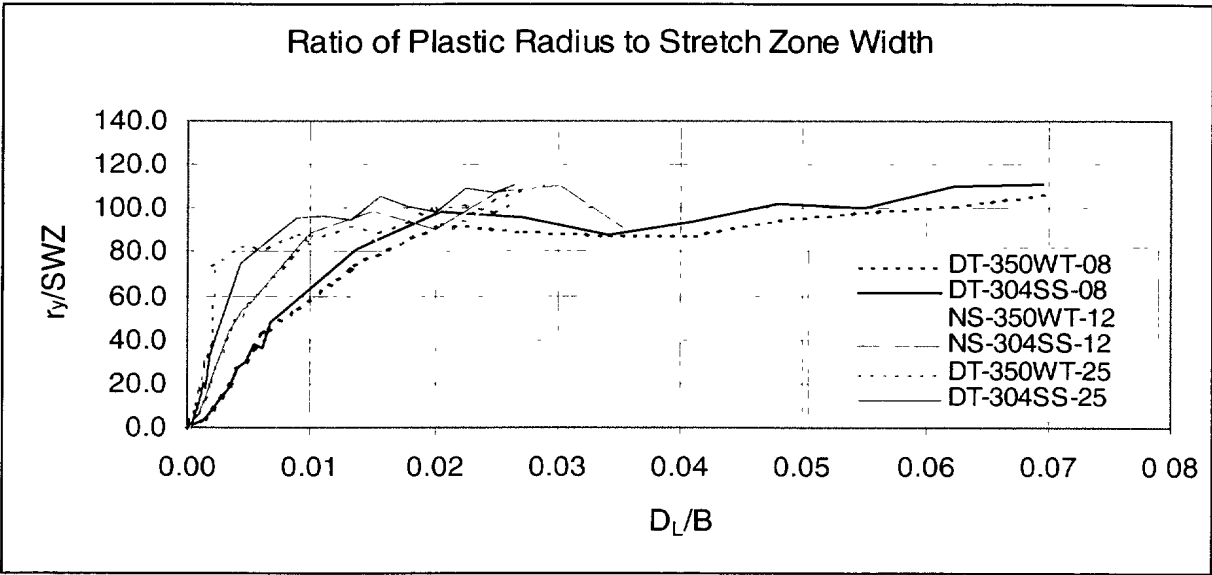
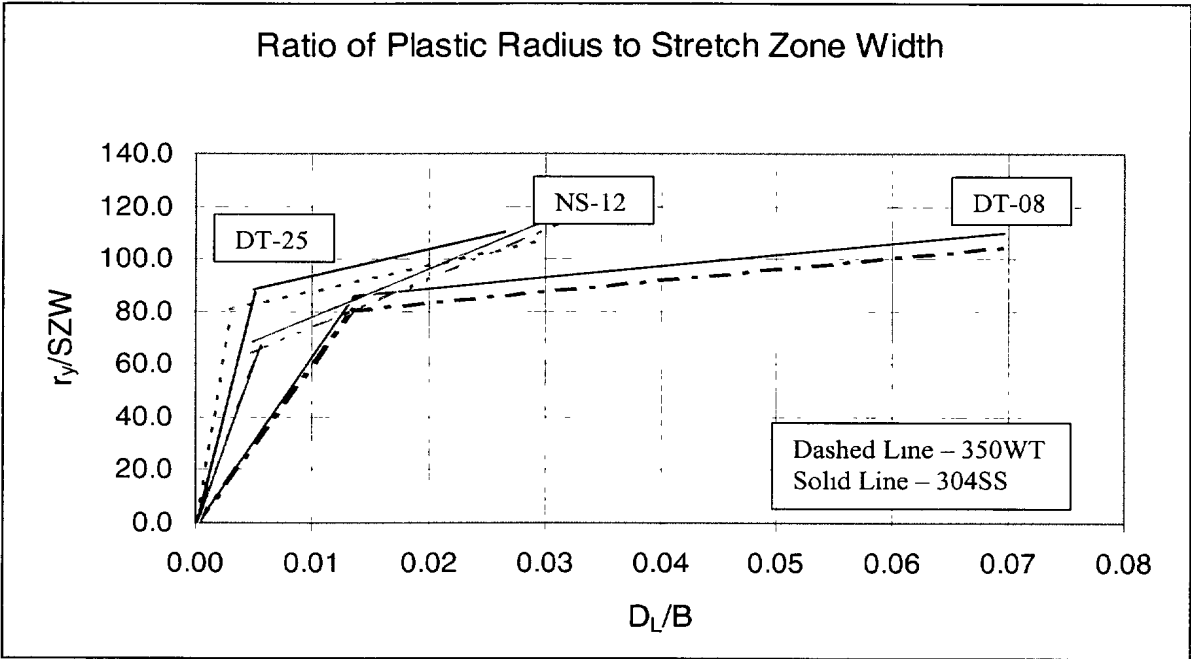


Figure 4.17: Variation of SZW with Non-Dimensionalized Displacement for all Specimens



(a)



(b)

Figure 4.18: Variation of  $r_y/SWZ$  with Non-Dimensionalized Displacement for all Specimens  
(a) Actual Data (b) Data Trend

## 5. SUMMARY, CONCLUSIONS AND RECOMMENDATIONS

### 5.1 Summary and Conclusions

This study is a continuation of efforts to investigate plastic zone development in three point bend fracture specimen. The finite element methodology was utilized to provide an understanding of the plastic zone size (radius) to crack tip blunting (stretch zone width), in order to be able to predict the upper limit where elastic plastic fracture becomes invalid. Finite element analysis of six test specimens were performed. The test specimens were (i) a standard dynamic tear DT test specimen with thickness of 8mm; (ii) a non-standard three point bend specimen with thickness of 12.5mm, and (iii) another DT specimen with thickness of 25mm; that were each made of 350WT and 304SS materials. The ABAQUS finite element code was used to perform incremental elastic-plastic analysis of the specimens.

The results computed included the progression of plastic strain, plastic radius ( $r_y$ ), stretch zone width (SZW), and the  $r_y$ /SZW ratio with plastic displacement. Contour plots of plastic strain and von Mises stresses presented at selected plastic displacement levels. The maximum plastic strain, plastic radius and SZW increased parabolically with the applied displacement. For a given non-dimensional displacement ( $D_L/B$ ), the maximum plastic strain as well as  $r_y$  and SZW increase with specimen thickness. Furthermore, it was observed that for a given specimen configuration, the  $r_y$  and SZW values are higher in the 350WT material than in the 304SS material.

Plots of the  $r_y$ /SZW ratios increase steadily and exhibit distinct points where the slopes change significantly. The curves fit bilinear trends lines very well. The slopes of the initial portions were always larger than those of the second parts of the bilinear curves. Furthermore, the slopes tend to increase with specimen thickness (or bending stiffness), and for a given specimen configuration, the slopes of the second portion of the curve for the 350WT and 304SS specimens were approximately equal although the  $r_y$ /SZW for the 304SS specimens were generally slightly higher than those of the 350WT material.

## 5.2 Recommendations

The experimental results on the plastic zone development in the specimens were not available to this study. It is recommended that the results of this study be compared to the experimental results when they are available. Based on these comparisons, it might be necessary to refine the methodology to obtain better accuracy. One area that needs further investigation is the effect of mesh size on the  $r_p/SZW$  ratio. Also, the effect of the 2-D modelling on the results should be investigated by performing some analyses on 3-D models. Such analysis would also provide information on the shear lip sizes.

## 6. REFERENCES

- [1] Koko, T.S., Gallant, B.K. and Tobin, S.M. "Investigation of Plastic Zone Development in Dynamic Tear Test Specimens." DREA, Contractor Report DREA-1999-095 July 1999.
- [2] Roy, V. Hyatt, C.V. and Matthews, J.R. "Precracking Stainless Steel 304 for Notch Tip Plastic Zone Studies." DREA Note No. DL(A)/98/1, 1998.
- [3] Hibbitt, H.D. Karlsson, B.I. and Sorensen, E.P. ABAQUS User's Manual, 1990.



**UNCLASSIFIED**  
 SECURITY CLASSIFICATION OF FORM  
 (highest classification of Title, Abstract, Keywords)

<b>DOCUMENT CONTROL DATA</b>		
(Security classification of title, body of abstract and indexing annotation must be entered when the overall document is classified)		
<b>1 ORIGINATOR</b> (the name and address of the organization preparing the document. Organizations for whom the document was prepared, e.g. Establishment sponsoring a contractor's report, or tasking agency, are entered in section 8.)  <b>Martec Ltd.</b> <b>400 – 1888 Brunswick Street</b> <b>Halifax NS B3J 3J8</b>	<b>2. SECURITY CLASSIFICATION</b> (overall security classification of the document including special warning terms if applicable)  <b>UNCLASSIFIED</b>	
<b>3 TITLE</b> (the complete document title as indicated on the title page. Its classification should be indicated by the appropriate abbreviation (S,C,R or U) in parentheses after the title)  <b>Investigation of Plastic Zone Development in Dynamic Tear Test Specimens – Phase II</b>		
<b>4. AUTHORS</b> (Last name, first name, middle initial. If military, show rank, e.g. Doe, Maj. John E.)  <b>T.S. Koko B.K. Gallant S.M. Tobin</b>		
<b>5 DATE OF PUBLICATION</b> (month and year of publication of document)  <b>September 2000</b>	<b>6a NO. OF PAGES</b> (total containing information. Include Annexes, Appendices, etc.)  <b>60 (approx.)</b>	<b>6b NO. OF REFS</b> (total cited in document)  <b>3</b>
<b>7 DESCRIPTIVE NOTES</b> (the category of the document, e.g. technical report, technical note or memorandum. If appropriate, enter the type of report, e.g. interim, progress, summary, annual or final. Give the inclusive dates when a specific reporting period is covered)  <b>CONTRACTOR REPORT</b>		
<b>8 SPONSORING ACTIVITY</b> (the name of the department project office or laboratory sponsoring the research and development. Include address) <b>Defence Research Establishment Atlantic</b> <b>PO Box 1012</b> <b>Dartmouth, NS, Canada B2Y 3Z7</b>		
<b>9a PROJECT OR GRANT NO.</b> (if appropriate, the applicable research and development project or grant number under which the document was written. Please specify whether project or grant)  <b>Project 1GH 36</b>	<b>9b CONTRACT NO.</b> (if appropriate, the applicable number under which the document was written)  <b>W7707-9-7208</b>	
<b>10a ORIGINATOR'S DOCUMENT NUMBER</b> (the official document number by which the document is identified by the originating activity. This number must be unique to this document.)	<b>10b OTHER DOCUMENT NOS.</b> (Any other numbers which may be assigned this document either by the originator or by the sponsor.)  <b>DREA CR 2000-115</b>	
<b>11 DOCUMENT AVAILABILITY</b> (any limitations on further dissemination of the document, other than those imposed by security classification) <input checked="" type="checkbox"/> <b>Unlimited distribution</b> <input type="checkbox"/> Defence departments and defence contractors; further distribution only as approved <input type="checkbox"/> Defence departments and Canadian defence contractors; further distribution only as approved <input type="checkbox"/> Government departments and agencies; further distribution only as approved <input type="checkbox"/> Defence departments; further distribution only as approved <input type="checkbox"/> Other (please specify):		
<b>12 DOCUMENT ANNOUNCEMENT</b> (any limitation to the bibliographic announcement of this document. This will normally correspond to the Document Availability (11). However, where further distribution (beyond the audience specified in (11)) is possible, a wider announcement audience may be selected.)		

**UNCLASSIFIED**  
 SECURITY CLASSIFICATION OF FORM  
**UNCLASSIFIED**  
 SECURITY CLASSIFICATION OF FORM

**UNCLASSIFIED**  
 SECURITY CLASSIFICATION OF FORM  
 (highest classification of Title, Abstract, Keywords)

13. **ABSTRACT** (a brief and factual summary of the document. It may also appear elsewhere in the body of the document itself. It is highly desirable that the abstract of classified documents be unclassified. Each paragraph of the abstract shall begin with an indication of the security classification of the information in the paragraph (unless the document itself is unclassified) represented as (S), (C), (R), or (U). It is not necessary to include here abstracts in both official languages unless the text is bilingual)

The development of the plastic zone in dynamic tear (DT) specimens and a non-standard three point bending fracture test specimen used to measure fracture properties was the main focus of the study. The ABAQUS finite element software was used to model the elastic-plastic behaviour of the specimens. For the DT specimen, a crack was induced by pressing the notch, followed by fatigue cracking at a limit load level of 40% of the specimen limit load, whereas, the crack shape for the non-standard specimen was a fatigue crack defined at approximately 30% of the limit load. The shapes of these cracks were adequately modelled in the finite element analysis. The specimens were made of 350WT steel and 304 stainless steel materials. The specimens were loaded until fixed amounts of permanent deformation were recorded. Results were obtained in the form of plots, showing the progression of the plastic zone around the crack tip. For each case, the results provide the following: mid point plastic deflection, stretch zone width and plastic zone radius. The finite element results obtained were compared to experimental elastic plastic testing where available, and reasonably accurate agreement was achieved.

14. **KEYWORDS, DESCRIPTORS or IDENTIFIERS** (technically meaningful terms or short phrases that characterize a document and could be helpful in cataloguing the document. They should be selected so that no security classification is required. Identifiers, such as equipment model designation, trade name, military project code name, geographic location may also be included. If possible keywords should be selected from a published thesaurus e.g. Thesaurus of Engineering and Scientific Terms (TEST) and that thesaurus-identified. If it not possible to select indexing terms which are Unclassified, the classification of each should be indicated as with the title)

plastic zone  
 dynamic tear (DT)  
 fracture properties  
 ABAQUS  
 finite element software  
 elastic-plastic behaviour  
 350WT steel  
 304 stainless steel  
 plastic zone around the crack tip  
 stretch zone width  
 plastic zone radius  
 finite element  
 elastic plastic

**UNCLASSIFIED**  
 SECURITY CLASSIFICATION OF FORM

The Defence Research  
and Development Branch  
provides Science and  
Technology leadership  
in the advancement and  
maintenance of Canada's  
defence capabilities.

Leader en sciences et  
technologie de la défense,  
la Direction de la recherche  
et du développement pour  
la défense contribue  
à maintenir et à  
accroître les compétences  
du Canada dans  
ce domaine.

#515214

